VEHICLE DYNAMICS IN CURRENTS

C. Woolsey

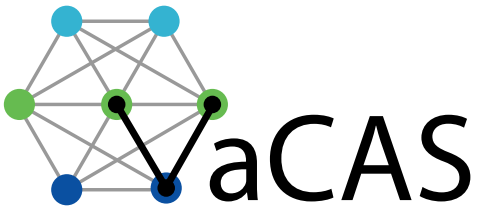

Virginia Center for Autonomous Systems
Virginia Polytechnic Institute & State University
Blacksburg, VA 24060
www.unmanned.vt.edu

September 30, 2011 (Revised March 9, 2012)

Technical Report No. VaCAS-2011-01

Summary

Vehicles operating in nonuniform flow fields are subject to forces and moments that are not captured by kinematic motion models. These effects are even greater when the mass of the displaced fluid is commensurate with the mass of the vehicle, as is the case for maritime vehicles and airships. Following along the lines of a recent paper by Thomasson, this report presents a dynamic model for the motion of a rigid vehicle in a nonuniform flow. The flow field is assumed to be irrotational, comprising a steady, nonuniform component and an unsteady, uniform component. As Thomasson suggests, rotational flow effects can be incorporated by modifying the vehicle's angular rate when computing viscous forces and moments. These equations have a variety of applications for modeling, simulation, and design, a few of which are listed at the end of the report.

Contents

List of Figures

List of Tables

1 Common Models

Table 1 summarizes four commonly used types of vehicle model, when the vehicle operates in an external flow field. As presented, the vehicle's inertial velocity (translational and/or rotational) is expressed in terms of the flow field velocity and the vehicle's *flow-relative* velocity. This approach emphasizes the role of relative flow; hydrodynamic effects such as lift and drag depend on the motion of the vehicle relative to the surrounding fluid. An alternative, but equivalent approach is to write the equations of motion in terms of the vehicle's *inertial* velocity. In this case, consistency of the dynamic models with Newton's second law is more transparent, but incorporating relative flow effects is a bit more cumbersome.

Motion Model & State Space	Equations
Kinematic Particle on $\mathbb{R}^3$	$\dot{\boldsymbol{X}} = \boldsymbol{v}_{\mathrm{f}}(\boldsymbol{X},t) + \boldsymbol{v}_{\mathrm{ctrl}}$
Dynamic Particle on $T\mathbb{R}^3$	$\left\{ \begin{array}{rcl} \dot{\boldsymbol{X}} & = & \boldsymbol{v}_{\mathrm{f}}(\boldsymbol{X},t) + \boldsymbol{v}_{\mathrm{r}} \\ m\dot{\boldsymbol{v}}_{\mathrm{r}} & = & \boldsymbol{f}_{\mathrm{o}}(\boldsymbol{X},\boldsymbol{v}_{\mathrm{r}},\boldsymbol{v}_{\mathrm{f}},t) + \boldsymbol{f}_{\mathrm{ctrl}} \end{array} \right\}$
Kinematic Body on $SE(3)$	$\left\{ \begin{array}{rcl} \dot{\boldsymbol{X}} & = & \boldsymbol{R}\left(\boldsymbol{v}_{\mathrm{f}}(\boldsymbol{X},t) + \boldsymbol{v}_{\mathrm{ctrl}}\right) \\ \dot{\boldsymbol{R}} & = & \boldsymbol{R}\hat{\boldsymbol{\omega}} \end{array} \right\}$
Dynamic Body on $TSE(3)$	$\left\{ \begin{array}{rcl} \dot{\boldsymbol{X}} & = & \boldsymbol{R}\left(\boldsymbol{v}_{\mathrm{f}}(\boldsymbol{X},t) + \boldsymbol{v}_{\mathrm{r}}\right) \\ \dot{\boldsymbol{R}} & = & \boldsymbol{R}\hat{\boldsymbol{\omega}} \\ \mathbb{M}\begin{pmatrix} \dot{\boldsymbol{v}}_{\mathrm{r}} \\ \dot{\boldsymbol{\omega}} \end{pmatrix} & = & \begin{pmatrix} \boldsymbol{f}_{\mathrm{o}}(\boldsymbol{X},\boldsymbol{R},\boldsymbol{v}_{\mathrm{r}},\boldsymbol{v}_{\mathrm{f}}(\boldsymbol{X},t),\boldsymbol{\omega},\boldsymbol{\omega}_{\mathrm{f}}(\boldsymbol{X},t)) + \boldsymbol{f}_{\mathrm{ctrl}} \\ \boldsymbol{m}_{\mathrm{o}}(\boldsymbol{X},\boldsymbol{R},\boldsymbol{v}_{\mathrm{r}},\boldsymbol{v}_{\mathrm{f}}(\boldsymbol{X},t),\boldsymbol{\omega},\boldsymbol{\omega}_{\mathrm{f}}(\boldsymbol{X},t)) + \boldsymbol{m}_{\mathrm{ctrl}} \end{pmatrix} \end{array} \right\}$

Table 1: Summary of basic motion models for a vehicle in a flow field. State variables include position ($\boldsymbol{X}(t) \in \mathbb{R}^3$), orientation ($\boldsymbol{R}(t) \in SO(3)$), body velocity ($\boldsymbol{v}(t) \in \mathbb{R}^3$), and body angular rate ($\boldsymbol{\omega}(t) \in \mathbb{R}^3$). Forces and moments are denoted $\boldsymbol{f}$ and $\boldsymbol{m}$, respectively. Subscripts indicate that terms pertain to the flow field ("f"), the control ("ctrl"), flow-relative motion ("r"), and other influences ("o"). The over-hat $\hat{\cdot}$ denotes the 3×3 skew-symmetric matrix satisfying $\hat{\boldsymbol{a}}\boldsymbol{b} = \boldsymbol{a} \times \boldsymbol{b}$ for 3-vectors $\boldsymbol{a}$ and $\boldsymbol{b}$. The 6×6 matrix $\mathbb{M}$ in the dynamic body model is the generalized rigid body inertia.

In the kinematic particle model it is assumed that the vehicle is a point mass and that velocity is an input. Currents appear as a perturbation to the input. For a "fully actuated particle" with sufficiently powerful actuators, the currents can be exactly canceled. If the vehicle is "weakly propelled," on the other hand, the ambient flow field dominates vehicle motion and the actuators are used only for small corrections. In these situations, interesting questions arise concerning the set of reachable states.

In the the dynamic particle model it is assumed that the vehicle is a point mass subject to a force input. This model is sometimes referred to as a "performance" model, since it is the appropriate setting for studying performance-related issues such as range and endurance. Here, the effect of currents appears both in the kinematic equations, which describe rates of change of *inertial* position and orientation, and in the dynamic equations.

The third model, the kinematic rigid body model, incorporates rotational degrees of freedom and includes angular velocity inputs. Again, currents appear as a perturbation to the input. In this case, the current field may include a rotational component to capture flow variations that occur on the scale of the vehicle's size. For example, a rigid vehicle located at the center of a Rankine vortex would experience a pure rotational disturbance due to the flow field.

Fourth, and most complicated, is the dynamic rigid body model. A careful treatment of dynamic modeling for a rigid vehicle in a flow field was presented by Thomasson [7]. The development follows Lamb's treatment of a rigid body moving through a perfect fluid (i.e., an inviscid and incompressible fluid) that is itself in motion. The volume of fluid may be accelerating and the treatment allows for flow gradients due to "cyclic irrotational" flow through a multiply connected region. Thomasson's modeling results are reviewed and amended here, although in different notation.

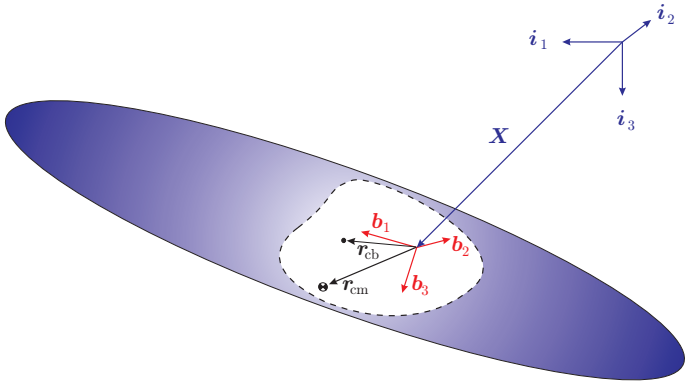

Figure 1: Reference frames.

2 A Rigid Vehicle in an Irrotational Flow Field

Consider a rigid vehicle of mass m which is fully immersed in a fluid of constant density. The vehicle displaces a volume of fluid of mass $\bar{m}$. If $m = \bar{m}$, then the vehicle is neutrally buoyant. More generally, if $\tilde{m} = m - \bar{m}$ is greater than zero, the vehicle is heavy in water and tends to sink while if $\tilde{m}$ is negative, the vehicle is buoyant in water and tends to rise. In some cases, the buoyancy may be adjusted through actuation, so that $\tilde{m}$ may be varied.

2.1 Kinematics

Let $\boldsymbol{X} = [\xi,\ \eta,\ \zeta]^T$ represent the position vector from the origin of an inertially fixed frame $\{\boldsymbol{i}_1, \boldsymbol{i}_2, \boldsymbol{i}_3\}$ to the origin of a body-fixed reference frame $\{\boldsymbol{b}_1, \boldsymbol{b}_2, \boldsymbol{b}_3\}$; see Figure 1. The vector $\boldsymbol{X}$ is expressed in the inertial frame. The orientation of the body is given by the rotation matrix $\boldsymbol{R}$, which maps free vectors from the body frame to the inertial frame. Let $\boldsymbol{v} = [u,\ v,\ w]^T$ and $\boldsymbol{\omega} = [p,\ q,\ r]^T$ represent the translational and rotational velocity of the body with respect to the inertial frame, but expressed in the body frame. The kinematic equations are

$$\dot{\boldsymbol{X}} = \boldsymbol{R}\boldsymbol{v} \tag{1}$$

$$\dot{\boldsymbol{R}} = \boldsymbol{R}\hat{\boldsymbol{\omega}} \tag{2}$$

where $\hat{\cdot}$ denotes the 3×3 skew-symmetric matrix satisfying $\hat{\boldsymbol{a}}\boldsymbol{b} = \boldsymbol{a} \times \boldsymbol{b}$ for vectors $\boldsymbol{a}$ and $\boldsymbol{b}$.

Following Thomasson [7], we consider a flow field comprising two components: a steady, circulating flow component $\boldsymbol{V}_{\mathrm{s}}(\boldsymbol{X})$ and an unsteady, but uniform flow component $\boldsymbol{V}_{\mathrm{s}}(\boldsymbol{X})$. Both are written as inertial vector fields over inertial space. In developing the vehicle dynamic equations, however,

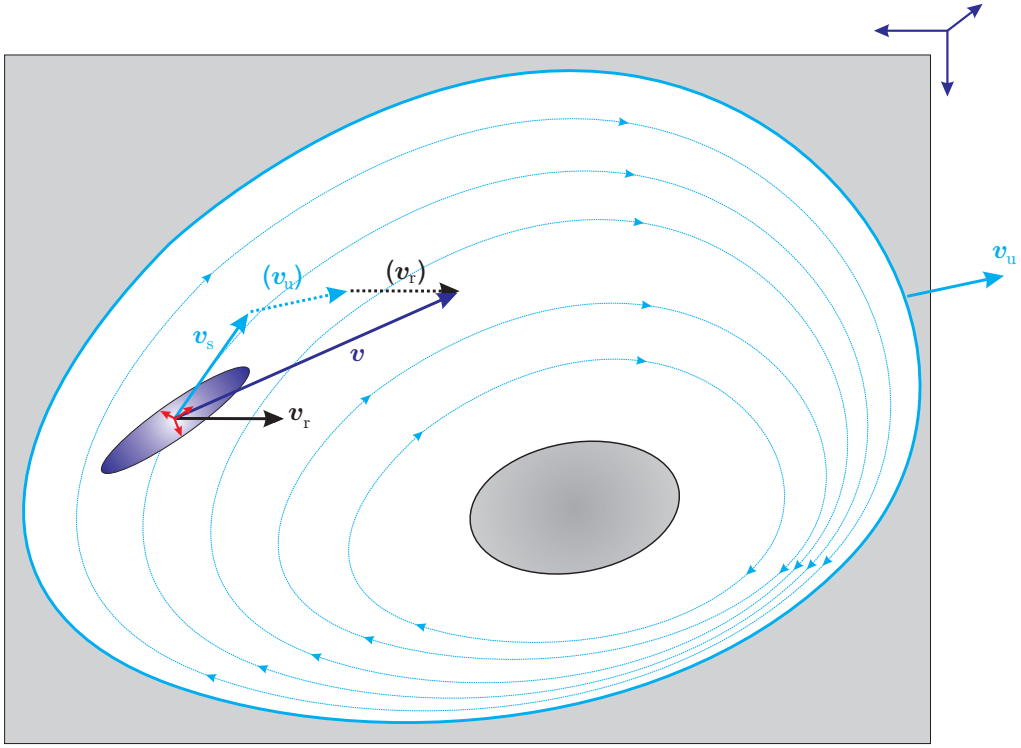

Figure 2: A rigid vehicle in a circulating flow contained in a translating vessel.

these two flow components are more conveniently expressed in the body-fixed reference frame. We therefore define

$$\boldsymbol{v}_{\mathrm{s}}(\boldsymbol{R},\boldsymbol{X}) = \boldsymbol{R}^T\boldsymbol{V}_{\mathrm{s}}(\boldsymbol{X}) \qquad \text{and} \qquad \boldsymbol{v}_{\mathrm{u}}(\boldsymbol{R},t) = \boldsymbol{R}^T\boldsymbol{V}_{\mathrm{u}}(t)$$

The complete flow field is

$$\boldsymbol{v}_{\mathrm{f}}(\boldsymbol{R},\boldsymbol{X},t) = \boldsymbol{v}_{\mathrm{s}}(\boldsymbol{R},\boldsymbol{X}) + \boldsymbol{v}_{\mathrm{u}}(\boldsymbol{R},t)$$

Note that $\boldsymbol{v}_{\mathrm{f}}(\boldsymbol{R},\boldsymbol{X},t) = \boldsymbol{0}$ does *not* imply that the fluid is at rest. Rather, it implies that the motion of the fluid is due solely to the body's motion through it, i.e., that there is no circulation and that the "containing vessel" is at rest (or translating at a constant speed). The ability to superimpose additional boundary conditions that allow for circulation and for translational acceleration is a consequence of the linearity of the governing partial differential equations.

2.2 Dynamics

The essential observation in deriving the equations of motion is that the system of impulsive pressures necessary to generate the vehicle and fluid motion from rest evolve according to a finite set of ordinary differential equations that derive from an expression of the vehicle/fluid system energy [3]. To express the system's kinetic energy, we must define the generalized inertia.

Consider a reference frame fixed in the vehicle. The vehicle's center of buoyancy (CB) is located at some point $\boldsymbol{r}_{\mathrm{cb}}$ with respect to the body reference frame and the center of mass (CM) is located at $\boldsymbol{r}_{\mathrm{cm}}$; see Figure 1. While Thomasson [7] allows for a general choice of reference frame, as indicated in the figure, we will assume that the CB is the origin of the body reference frame, so that $\boldsymbol{r}_{\mathrm{cb}} = \boldsymbol{0}$.

It is straightforward to account for an offset CB, but the additional detail unnecessarily complicates the presentation. On the other hand, we must generally assume that the vehicle's CM is displaced from its CB: $\boldsymbol{r}_{\rm cm} \neq \boldsymbol{0}$

Let

$$\boldsymbol{\nu} = \begin{pmatrix} \boldsymbol{v} \\ \boldsymbol{\omega} \end{pmatrix}, \qquad \boldsymbol{\nu}_{\rm u} = \begin{pmatrix} \boldsymbol{v}_{\rm u} \\ \boldsymbol{0} \end{pmatrix} \qquad \text{and} \qquad \boldsymbol{\nu}_{\rm s} = \begin{pmatrix} \boldsymbol{v}_{\rm s} \\ \boldsymbol{0} \end{pmatrix}$$

We also denote the generalized velocity of the vehicle relative to the flow as follows:

$$\boldsymbol{\nu}_{\rm r} = \begin{pmatrix} \boldsymbol{v}_{\rm r} \\ \boldsymbol{\omega} \end{pmatrix} \qquad \text{where} \qquad \boldsymbol{v}_{\rm r} = \boldsymbol{v} - \boldsymbol{v}_{\rm u} - \boldsymbol{v}_{\rm s}$$

If $\boldsymbol{I}_{\rm rb}$ denotes the 3×3 matrix of moments and products of inertia for the rigid vehicle, then the 6×6 "generalized inertia" matrix for the rigid vehicle is

$$\mathbb{M} = \begin{pmatrix} m\mathbb{I} & -m\hat{\boldsymbol{r}}_{\rm cm} \\ m\hat{\boldsymbol{r}}_{\rm cm} & \boldsymbol{I}_{\rm rb} \end{pmatrix}$$

where $\mathbb{I}$ is the 3×3 identity matrix. The kinetic energy of the rigid vehicle is $\frac{1}{2}\boldsymbol{\nu}^T \mathbb{M} \boldsymbol{\nu}$.

Let $\mathbb{M}_{\rm f}$ denote the 6×6 matrix of "added mass and inertia" parameters, which account for the energy necessary to accelerate the fluid around the vehicle as it moves. Under the given assumptions of a rigid vehicle immersed in an inviscid, incompressible fluid, the elements of $\mathbb{M}_{\rm f}$ are constant volume integrals that depend only on the vehicle shape and the fluid density. In the final equations, these parameters account for the impulsive pressures necessary to generate a given motion of the vehicle/fluid system in the case where $\boldsymbol{v}_{\rm f}(\boldsymbol{R}, \boldsymbol{X}, t) = \boldsymbol{0}$.

We also define the following 6×6 matrix to account for the kinetic energy of the fluid that is replaced by the vehicle:

$$\bar{\mathbb{M}} = \begin{pmatrix} \bar{m}\mathbb{I} & \boldsymbol{0} \\ \boldsymbol{0} & \boldsymbol{0} \end{pmatrix}$$

The underlying assumption, noted in [3] and in [7], is that spatial variations in the flow field due to circulation (that is, the variations in $\boldsymbol{V}_{\rm s}(\boldsymbol{X})$) are negligible over the scale of the vehicle. It is therefore appropriate to treat the vehicle-shaped pocket as a neutrally buoyant body with no inertia. The distinction between an "inertia-less body" and a particle is important; though the vehicle-shaped pocket stores no rotational kinetic energy, its (rigid) exterior shape provides boundary conditions for the flow equations.

Following [7], we write the kinetic energy of the combined fluid/vehicle system as follows:

$$T = \underbrace{K + \frac{1}{2} M \boldsymbol{\nu}_{\rm u}^T \boldsymbol{\nu}_{\rm u}}_{\substack{\text{fluid energy,} \\ \text{absent the vehicle}}} + \underbrace{\frac{1}{2} \boldsymbol{\nu}_{\rm r}^T \left(\mathbb{M}_{\rm f} + \bar{\mathbb{M}} \right) \boldsymbol{\nu}_{\rm r}}_{\substack{\text{energy due to motion of} \\ \text{fluid-filled hullform}}} + \underbrace{\frac{1}{2} \boldsymbol{\nu}^T \mathbb{M} \boldsymbol{\nu}}_{\substack{\text{vehicle} \\ \text{energy}}} - \underbrace{\frac{1}{2} \boldsymbol{\nu}^T \bar{\mathbb{M}} \boldsymbol{\nu}}_{\substack{\text{energy of (absent)} \\ \text{fluid-filled hullform}}}$$

The term K accounts for the kinetic energy necessary to establish the circulating motion in the fluid volume; see Chapter 6 of Lamb [3]. The parameter M represents the mass of the complete volume of fluid (before any is replaced by the vehicle). Neither term ultimately appears in the dynamic equations describing the vehicle motion. Note, in the case that $\boldsymbol{v}_{\rm f}(\boldsymbol{R}, \boldsymbol{X}, t) = \boldsymbol{0}$, the kinetic energy of the vehicle/fluid system is simply

$$T = \frac{1}{2} \boldsymbol{\nu}^T (\mathbb{M} + \mathbb{M}_{\rm f}) \boldsymbol{\nu}.$$

The equations for the more general case can be derived using Lagrangian mechanics. Anticipating that the final equations will be most conveniently expressed in the body-fixed reference frame, we follow Thomasson's approach [7] and use the artifice of "quasi-coordinates" – fictitious coordinates whose time derivatives are body frame velocities (e.g., the components of $\boldsymbol{v}$ and $\boldsymbol{\omega}$).

Quasicoordinates. Let

$$\mathcal{L}(\boldsymbol{q}, \dot{\boldsymbol{q}}, t) = T(\boldsymbol{q}, \dot{\boldsymbol{q}}, t) - V(\boldsymbol{q})$$

be the Lagrangian for a mechanical system with generalized coordinates $\boldsymbol{q}$. Lagrange's equations are

$$\frac{d}{dt}\frac{\partial \mathcal{L}}{\partial \dot{\boldsymbol{q}}} - \frac{\partial \mathcal{L}}{\partial \boldsymbol{q}} = \boldsymbol{Q}$$

where $\boldsymbol{Q}$ represents generalized exogenous forces.

Suppose we wish to express the Lagrangian in alternative variables $(\boldsymbol{q}, \boldsymbol{\varpi})$ where the alternative velocity variables $\boldsymbol{\varpi}$ may not correspond to time derivatives of any configuration variables. (A classic example, as discussed by Schaub and Junkins [6], is the body angular rate vector for a rotating spacecraft.) We assume that it is possible to write

$$\dot{\boldsymbol{q}} = \boldsymbol{D}(\boldsymbol{q})\boldsymbol{\varpi}$$

so that by simple substitution we obtain a new Lagrangian

$$\bar{\mathcal{L}}(\boldsymbol{q}, \boldsymbol{\varpi}, t) = \mathcal{L}(\boldsymbol{q}, \boldsymbol{D}(\boldsymbol{q})\boldsymbol{\varpi}, t)$$

The alternate form of Lagrange's equations, using this modified Lagrangian, is

$$\frac{d}{dt}\frac{\partial \bar{\mathcal{L}}}{\partial \boldsymbol{\varpi}} + \boldsymbol{G}(\boldsymbol{q}, \boldsymbol{\varpi})\frac{\partial \bar{\mathcal{L}}}{\partial \boldsymbol{\varpi}} - \boldsymbol{D}(\boldsymbol{q})^T \frac{\partial \bar{\mathcal{L}}}{\partial \boldsymbol{q}} = \boldsymbol{D}(\boldsymbol{q})^T \boldsymbol{Q} \tag{3}$$

where the elements of the matrix $\boldsymbol{G}(\boldsymbol{q}, \boldsymbol{\varpi})$ are [6]

$$G_{ij} = \sum_{k=1}^{n}\sum_{l=1}^{n}\sum_{m=1}^{n} D_{ki} D_{lm} \varpi_m \left(\frac{\partial D_{kj}^{-T}}{q_l} - \frac{\partial D_{lj}^{-T}}{q_k} \right) \tag{4}$$

and D_{kj}^{-T} denotes the kj^{th} element of the matrix

$$\boldsymbol{D}(\boldsymbol{q})^{-T} = (\boldsymbol{D}(\boldsymbol{q})^T)^{-1} = (\boldsymbol{D}(\boldsymbol{q})^{-1})^T$$

Define generalized coordinates

$$\boldsymbol{q} = \begin{pmatrix} \boldsymbol{X} \\ \boldsymbol{\Theta} \end{pmatrix} \tag{5}$$

where $\boldsymbol{X}$ and $\boldsymbol{\Theta}$ represent the inertial position and orientation of the vehicle using, for example, north-east-down coordinates for position and Euler angles for orientation. For a given state history, the position $\boldsymbol{X}$ evolves according to equation (1) while the orientation evolves according to equation (2), but with $\boldsymbol{R}(\boldsymbol{\Theta})$ parameterized by Euler angles. Equations (1) and (2) become

$$\begin{aligned} \dot{\boldsymbol{X}} &= \boldsymbol{R}(\boldsymbol{\Theta})\boldsymbol{v} \\ \dot{\boldsymbol{\Theta}} &= \boldsymbol{L}(\boldsymbol{\Theta})\boldsymbol{\omega} \end{aligned}$$

Explicit expressions for the rotation matrix $\boldsymbol{R}(\boldsymbol{\Theta})$ and the transformation $\boldsymbol{L}(\boldsymbol{\Theta})$ can be found in any textbook on vehicle dynamics; see [1] or [2], for example.

Because we wish to express the dynamic equations in the body frame, we define "quasi-coordinates" such that the quasi-coordinate velocity vector is $\boldsymbol{\varpi} = \boldsymbol{\nu}$. The quasi-coordinate velocity is related to the generalized velocity as follows:

$$\dot{\boldsymbol{q}} = \underbrace{\text{diag}\left(\boldsymbol{R}(\boldsymbol{\Theta}), \boldsymbol{L}(\boldsymbol{\Theta})\right)}_{\boldsymbol{D}(\boldsymbol{q})} \boldsymbol{\nu} \tag{6}$$

According to equation (4), one finds that

$$\boldsymbol{G}(\boldsymbol{q}, \boldsymbol{\nu}) = \begin{pmatrix} \hat{\boldsymbol{\omega}} & \boldsymbol{0} \\ \hat{\boldsymbol{v}} & \hat{\boldsymbol{\omega}} \end{pmatrix}$$

To determine the dynamics using equation (3), with

$$\begin{aligned} \bar{\mathcal{L}}(\boldsymbol{q}, \boldsymbol{\nu}, t) &= K + \frac{1}{2} M \boldsymbol{\nu}_{\text{u}}^T \boldsymbol{\nu}_{\text{u}} + \frac{1}{2} \left(\boldsymbol{\nu} - \boldsymbol{\nu}_{\text{u}} - \boldsymbol{\nu}_{\text{s}}\right)^T \left(\mathbb{M}_{\text{f}} + \bar{\mathbb{M}}\right) \left(\boldsymbol{\nu} - \boldsymbol{\nu}_{\text{u}} - \boldsymbol{\nu}_{\text{s}}\right) \\ &\quad + \frac{1}{2} \boldsymbol{\nu}^T \mathbb{M} \boldsymbol{\nu} - \frac{1}{2} \boldsymbol{\nu}^T \bar{\mathbb{M}} \boldsymbol{\nu}, \end{aligned}$$

we first compute

$$\frac{\partial \bar{\mathcal{L}}}{\partial \boldsymbol{\nu}} = \left(\mathbb{M}_{\text{f}} + \mathbb{M}\right) \boldsymbol{\nu} - \left(\mathbb{M}_{\text{f}} + \bar{\mathbb{M}}\right) \left(\boldsymbol{\nu}_{\text{u}} + \boldsymbol{\nu}_{\text{s}}\right)$$

Differentiating with respect to time, we find

$$\frac{d}{dt} \frac{\partial \bar{\mathcal{L}}}{\partial \boldsymbol{\nu}} = \left(\mathbb{M}_{\text{f}} + \mathbb{M}\right) \dot{\boldsymbol{\nu}} - \left(\mathbb{M}_{\text{f}} + \bar{\mathbb{M}}\right) \begin{pmatrix} \frac{d}{dt}(\boldsymbol{v}_{\text{u}} + \boldsymbol{v}_{\text{s}}) \\ \boldsymbol{0} \end{pmatrix}$$

Differentiating the flow velocities, we have

$$\begin{aligned} \frac{d}{dt} \left(\boldsymbol{v}_{\text{u}} + \boldsymbol{v}_{\text{s}}\right) &= \frac{d}{dt} \left[\boldsymbol{R}^T \left(\boldsymbol{V}_{\text{u}}(t) + \boldsymbol{V}_{\text{s}}(\boldsymbol{X})\right)\right] \\ &= \left(\boldsymbol{R}\hat{\boldsymbol{\omega}}\right)^T \left(\boldsymbol{V}_{\text{u}}(t) + \boldsymbol{V}_{\text{s}}(\boldsymbol{X})\right) + \boldsymbol{R}^T \left(\dot{\boldsymbol{V}}_{\text{u}} + \frac{\partial \boldsymbol{V}_{\text{s}}}{\partial \boldsymbol{X}} \dot{\boldsymbol{X}}\right) \\ &= -\hat{\boldsymbol{\omega}} \left(\boldsymbol{v}_{\text{u}} + \boldsymbol{v}_{\text{s}}\right) + \frac{\partial}{\partial t} \boldsymbol{v}_{\text{u}} + \boldsymbol{R}^T \frac{\partial \boldsymbol{V}_{\text{s}}}{\partial \boldsymbol{X}} \boldsymbol{R} \boldsymbol{v} \end{aligned} \tag{7}$$

Thus,

$$\frac{d}{dt} \frac{\partial \bar{\mathcal{L}}}{\partial \boldsymbol{\nu}} = \left(\mathbb{M}_{\text{f}} + \mathbb{M}\right) \dot{\boldsymbol{\nu}} - \left(\mathbb{M}_{\text{f}} + \bar{\mathbb{M}}\right) \begin{pmatrix} \left(\boldsymbol{v}_{\text{u}} + \boldsymbol{v}_{\text{s}}\right) \times \boldsymbol{\omega} + \frac{\partial}{\partial t} \boldsymbol{v}_{\text{u}} + \boldsymbol{R}^T \frac{\partial \boldsymbol{V}_{\text{s}}}{\partial \boldsymbol{X}} \boldsymbol{R} \boldsymbol{v} \\ \boldsymbol{0} \end{pmatrix}$$

Next, we compute $\frac{\partial \bar{\mathcal{L}}}{\partial \boldsymbol{q}}$. In doing so, the following identity proves quite useful:

$$\frac{\partial}{\partial \boldsymbol{y}} \left(\frac{1}{2} \boldsymbol{z}(\boldsymbol{y})^T \boldsymbol{Q} \boldsymbol{z}(\boldsymbol{y})\right) = \left(\frac{\partial \boldsymbol{z}}{\partial \boldsymbol{y}}\right)^T \boldsymbol{Q} \boldsymbol{z}(\boldsymbol{y}),$$

It is also useful to note that

$$\frac{d}{d\Theta_i} \boldsymbol{R}(\boldsymbol{\Theta}) = \boldsymbol{R}(\boldsymbol{\Theta}) \widehat{\boldsymbol{L}(\boldsymbol{\Theta})^{-1}} \boldsymbol{e}_i$$

where Θ_i is the i^{th} element of $\boldsymbol{\Theta}$ and $\boldsymbol{e}_i$ is the i^{th} basis vector for $\mathbb{R}^3$ (e.g., $\boldsymbol{e}_1 = [1,0,0]^T$). Recognizing that the only dependence of the Lagrangian on configuration variables is through the terms $\boldsymbol{v}_{\text{u}}(\boldsymbol{R},t)$ and $\boldsymbol{v}_{\text{s}}(\boldsymbol{R},\boldsymbol{X})$, and using the identities above, we compute

$$\frac{\partial \bar{\mathcal{L}}}{\partial \boldsymbol{q}} = -\begin{pmatrix} \left(\frac{\partial \boldsymbol{V}_{\text{s}}}{\partial \boldsymbol{X}}\right)^T \boldsymbol{R} & \boldsymbol{0} \\ \boldsymbol{L}^{-T}(\hat{\boldsymbol{v}}_{\text{u}} + \hat{\boldsymbol{v}}_{\text{s}}) & \boldsymbol{0} \end{pmatrix} \left(\mathbb{M}_{\text{f}} + \bar{\mathbb{M}}\right)(\boldsymbol{\nu} - \boldsymbol{\nu}_{\text{u}} - \boldsymbol{\nu}_{\text{s}})$$

Referring to equation (3), we find that

$$\begin{aligned} -\boldsymbol{D}(\boldsymbol{q})^T \frac{\partial \bar{\mathcal{L}}}{\partial \boldsymbol{q}} &= \begin{pmatrix} \boldsymbol{R}^T & \boldsymbol{0} \\ \boldsymbol{0} & \boldsymbol{L}^T \end{pmatrix} \begin{pmatrix} \left(\frac{\partial \boldsymbol{V}_{\text{s}}}{\partial \boldsymbol{X}}\right)^T \boldsymbol{R} & \boldsymbol{0} \\ \boldsymbol{L}^{-T}(\hat{\boldsymbol{v}}_{\text{u}} + \hat{\boldsymbol{v}}_{\text{s}}) & \boldsymbol{0} \end{pmatrix} \left(\mathbb{M}_{\text{f}} + \bar{\mathbb{M}}\right)(\boldsymbol{\nu} - \boldsymbol{\nu}_{\text{u}} - \boldsymbol{\nu}_{\text{s}}) \\ &= \begin{pmatrix} \boldsymbol{R}^T \left(\frac{\partial \boldsymbol{V}_{\text{s}}}{\partial \boldsymbol{X}}\right)^T \boldsymbol{R} & \boldsymbol{0} \\ (\hat{\boldsymbol{v}}_{\text{u}} + \hat{\boldsymbol{v}}_{\text{s}}) & \boldsymbol{0} \end{pmatrix} \left(\mathbb{M}_{\text{f}} + \bar{\mathbb{M}}\right)(\boldsymbol{\nu} - \boldsymbol{\nu}_{\text{u}} - \boldsymbol{\nu}_{\text{s}}) \end{aligned}$$

The complete vehicle dynamics are

$$\begin{aligned} &\left[\left(\mathbb{M}_{\text{f}} + \mathbb{M}\right)\dot{\boldsymbol{\nu}} - \left(\mathbb{M}_{\text{f}} + \bar{\mathbb{M}}\right)\begin{pmatrix} (\boldsymbol{v}_{\text{u}} + \boldsymbol{v}_{\text{s}}) \times \boldsymbol{\omega} + \frac{\partial}{\partial t}\boldsymbol{v}_{\text{u}} + \boldsymbol{R}^T \frac{\partial \boldsymbol{V}_{\text{s}}}{\partial \boldsymbol{X}} \boldsymbol{R}\boldsymbol{v} \\ \boldsymbol{0} \end{pmatrix}\right] \\ &\quad + \left[\begin{pmatrix} \hat{\boldsymbol{\omega}} & \boldsymbol{0} \\ \hat{\boldsymbol{v}} & \hat{\boldsymbol{\omega}} \end{pmatrix}\left(\left(\mathbb{M}_{\text{f}} + \mathbb{M}\right)\boldsymbol{\nu} - \left(\mathbb{M}_{\text{f}} + \bar{\mathbb{M}}\right)(\boldsymbol{\nu}_{\text{u}} + \boldsymbol{\nu}_{\text{s}})\right)\right] \\ &\quad + \begin{pmatrix} \boldsymbol{R}^T \left(\frac{\partial \boldsymbol{V}_{\text{s}}}{\partial \boldsymbol{X}}\right)^T \boldsymbol{R} & \boldsymbol{0} \\ (\hat{\boldsymbol{v}}_{\text{u}} + \hat{\boldsymbol{v}}_{\text{s}}) & \boldsymbol{0} \end{pmatrix}\left(\mathbb{M}_{\text{f}} + \bar{\mathbb{M}}\right)(\boldsymbol{\nu} - \boldsymbol{\nu}_{\text{u}} - \boldsymbol{\nu}_{\text{s}}) = \begin{pmatrix} \boldsymbol{f} \\ \boldsymbol{m} \end{pmatrix} \end{aligned} \tag{8}$$

where $\boldsymbol{f}$ and $\boldsymbol{m}$ represent exogenous forces and moments, respectively, that account for gravitational effects, control effects, viscous damping, and other influences that are not accounted for explicitly within the Lagrangian formulation.

Remark 2.1 *In [7], the steady, circulating flow component $\boldsymbol{v}_{\text{s}}$ is treated as a function of the* quasi-coordinates *that define position relative to the body frame. The matrix*

$$\boldsymbol{\Phi}^T = \left(\frac{\partial \boldsymbol{v}_{\text{s}}}{\partial \boldsymbol{X}}\right)\boldsymbol{R} = \boldsymbol{R}^T\left(\frac{\partial \boldsymbol{V}_{\text{s}}}{\partial \boldsymbol{X}}\right)\boldsymbol{R} \tag{9}$$

appearing in [7] is the Jacobian of $\boldsymbol{v}_{\text{s}}$ with respect to these quasi-coordinates. Note that this flow gradient term, or its transpose, appears in the first and third lines of (8). Importantly, in this paper this matrix is not symmetric since the flow can contain vorticity.

Rearranging terms in (8), and using the notation introduced in Remark 2.1, one obtains the vehicle dynamic equations in terms of the inertial velocity:

$$\begin{aligned} \left(\mathbb{M}_{\text{f}} + \mathbb{M}\right)\dot{\boldsymbol{\nu}} &= -\begin{pmatrix} \hat{\boldsymbol{\omega}} + \boldsymbol{\Phi} & \boldsymbol{0} \\ \hat{\boldsymbol{v}} - \hat{\boldsymbol{v}}_{\text{u}} - \hat{\boldsymbol{v}}_{\text{s}} & \hat{\boldsymbol{\omega}} \end{pmatrix}\left(\mathbb{M}_{\text{f}} + \bar{\mathbb{M}}\right)(\boldsymbol{\nu} - \boldsymbol{\nu}_{\text{u}} - \boldsymbol{\nu}_{\text{s}}) - \begin{pmatrix} \hat{\boldsymbol{\omega}} & \boldsymbol{0} \\ \hat{\boldsymbol{v}} & \hat{\boldsymbol{\omega}} \end{pmatrix}\left(\mathbb{M} - \bar{\mathbb{M}}\right)\boldsymbol{\nu} \\ &\quad + \left(\mathbb{M}_{\text{f}} + \bar{\mathbb{M}}\right)\begin{pmatrix} (\boldsymbol{v}_{\text{u}} + \boldsymbol{v}_{\text{s}}) \times \boldsymbol{\omega} + \frac{\partial}{\partial t}\boldsymbol{v}_{\text{u}} + \boldsymbol{\Phi}^T\boldsymbol{v} \\ \boldsymbol{0} \end{pmatrix} + \begin{pmatrix} \boldsymbol{f} \\ \boldsymbol{m} \end{pmatrix} \end{aligned} \tag{10}$$

Remark 2.2 *Recall from (7) that the expression*

$$(\boldsymbol{v}_{\mathrm{u}} + \boldsymbol{v}_{\mathrm{s}}) \times \boldsymbol{\omega} + \frac{\partial}{\partial t}\boldsymbol{v}_{\mathrm{u}} + \boldsymbol{\Phi}^T \boldsymbol{v}$$

is the total time derivative of the flow field, expressed in the body frame. The third term plays an especially important role in nonuniform flows, as discussed in Section 2.3. This term was omitted in [7], due to an editing error, but was correctly included in [8]. There is a subtle distinction between the expression given above and the corresponding expression in [8]; the earlier paper expressed the gradient matrix $\boldsymbol{\Phi}$ *relative to coordinates fixed in the (uniformly accelerating) containing vessel, rather than inertial coordinates.*

Flow-relative dynamic equations. Equations (10) describe the evolution of the vehicle's inertial velocity. To obtain the equations relative to the flow, we subtract

$$(\mathbb{M}_{\mathrm{f}} + \mathbb{M})\,(\dot{\boldsymbol{\nu}}_{\mathrm{u}} + \dot{\boldsymbol{\nu}}_{\mathrm{s}}) = (\mathbb{M}_{\mathrm{f}} + \mathbb{M}) \begin{pmatrix} (\boldsymbol{v}_{\mathrm{u}} + \boldsymbol{v}_{\mathrm{s}}) \times \boldsymbol{\omega} + \frac{\partial}{\partial t}\boldsymbol{v}_{\mathrm{u}} + \boldsymbol{\Phi}^T \boldsymbol{v} \\ \mathbf{0} \end{pmatrix}$$

from equation (10) to obtain:

$$\begin{aligned} (\mathbb{M}_{\mathrm{f}} + \mathbb{M})\,\dot{\boldsymbol{\nu}}_{\mathrm{r}} \;=\; & -\begin{pmatrix} \hat{\boldsymbol{\omega}} + \boldsymbol{\Phi} & \mathbf{0} \\ \hat{\boldsymbol{v}}_{\mathrm{r}} & \hat{\boldsymbol{\omega}} \end{pmatrix} (\mathbb{M}_{\mathrm{f}} + \bar{\mathbb{M}})\,\boldsymbol{\nu}_{\mathrm{r}} - \begin{pmatrix} \hat{\boldsymbol{\omega}} & \mathbf{0} \\ \hat{\boldsymbol{v}} & \hat{\boldsymbol{\omega}} \end{pmatrix} (\mathbb{M} - \bar{\mathbb{M}})\,\boldsymbol{\nu} \\ & + (\bar{\mathbb{M}} - \mathbb{M}) \begin{pmatrix} (\boldsymbol{v}_{\mathrm{u}} + \boldsymbol{v}_{\mathrm{s}}) \times \boldsymbol{\omega} + \frac{\partial}{\partial t}\boldsymbol{v}_{\mathrm{u}} + \boldsymbol{\Phi}^T \boldsymbol{v} \\ \mathbf{0} \end{pmatrix} + \begin{pmatrix} \boldsymbol{f} \\ \boldsymbol{m} \end{pmatrix} \end{aligned} \tag{11}$$

Rearranging terms, as described in Appendix A,

$$\begin{aligned} (\mathbb{M}_{\mathrm{f}} + \mathbb{M})\,\dot{\boldsymbol{\nu}}_{\mathrm{r}} = & -\begin{pmatrix} \hat{\boldsymbol{\omega}} & \mathbf{0} \\ \hat{\boldsymbol{v}}_{\mathrm{r}} & \hat{\boldsymbol{\omega}} \end{pmatrix} (\mathbb{M}_{\mathrm{f}} + \mathbb{M})\,\boldsymbol{\nu}_{\mathrm{r}} + \begin{pmatrix} \boldsymbol{f} \\ \boldsymbol{m} \end{pmatrix} \\ & - \begin{pmatrix} \hat{\boldsymbol{\omega}} & \mathbf{0} \\ \hat{\boldsymbol{v}}_{\mathrm{r}} + \hat{\boldsymbol{v}}_{\mathrm{u}} + \hat{\boldsymbol{v}}_{\mathrm{s}} & \hat{\boldsymbol{\omega}} \end{pmatrix} (\mathbb{M} - \bar{\mathbb{M}}) \begin{pmatrix} \boldsymbol{v}_{\mathrm{u}} + \boldsymbol{v}_{\mathrm{s}} \\ \mathbf{0} \end{pmatrix} - \begin{pmatrix} \mathbf{0} & \mathbf{0} \\ \hat{\boldsymbol{v}}_{\mathrm{u}} + \hat{\boldsymbol{v}}_{\mathrm{s}} & \mathbf{0} \end{pmatrix} (\mathbb{M} - \bar{\mathbb{M}})\,\boldsymbol{\nu}_{\mathrm{r}} \\ & - (\mathbb{M} - \bar{\mathbb{M}}) \begin{pmatrix} (\boldsymbol{v}_{\mathrm{u}} + \boldsymbol{v}_{\mathrm{s}}) \times \boldsymbol{\omega} + \frac{\partial}{\partial t}\boldsymbol{v}_{\mathrm{u}} + \boldsymbol{\Phi}^T (\boldsymbol{v}_{\mathrm{r}} + \boldsymbol{v}_{\mathrm{u}} + \boldsymbol{v}_{\mathrm{s}}) \\ \mathbf{0} \end{pmatrix} - \begin{pmatrix} \boldsymbol{\Phi} & \mathbf{0} \\ \mathbf{0} & \mathbf{0} \end{pmatrix} (\mathbb{M}_{\mathrm{f}} + \bar{\mathbb{M}})\,\boldsymbol{\nu}_{\mathrm{r}} \end{aligned} \tag{12}$$

If there is no flow, then only the terms in the first line remain. Fossen suggests that the first line of (12) also provides a sufficient approximation for external flow effects in slowly varying currents [2, Eqn. (3.11), pg. 59]. If the vehicle is neutrally buoyant ($m = \bar{m}$) and the CM coincides with the CB ($\boldsymbol{r}_{\mathrm{cm}} = \mathbf{0}$), then the second line of (12) vanishes, along with the first term in the third line. If the flow is uniform, the final term vanishes, as well. Under these conditions, the approximation suggested by Fossen is exact.

2.3 Reprise of Thomasson's Equations

Here, we recall Thomasson's equations of motion (equation (52) in [7], with $\boldsymbol{r}_{\mathrm{cb}} = \mathbf{0}$):

$$\begin{aligned} (\mathbb{M}_{\mathrm{f}} + \mathbb{M})\,\dot{\boldsymbol{\nu}} \;=\; & -\begin{pmatrix} \hat{\boldsymbol{\omega}} & \mathbf{0} \\ \hat{\boldsymbol{v}}_{\mathrm{r}} & \hat{\boldsymbol{\omega}} \end{pmatrix} (\mathbb{M}_{\mathrm{f}} + \bar{\mathbb{M}})\,\boldsymbol{\nu}_{\mathrm{r}} - \begin{pmatrix} \hat{\boldsymbol{\omega}} & \mathbf{0} \\ \hat{\boldsymbol{v}} & \hat{\boldsymbol{\omega}} \end{pmatrix} (\mathbb{M} - \bar{\mathbb{M}})\,\boldsymbol{\nu} + \begin{pmatrix} \boldsymbol{f} \\ \boldsymbol{m} \end{pmatrix} \\ & + (\mathbb{M}_{\mathrm{f}} + \bar{\mathbb{M}}) \begin{pmatrix} \dot{\boldsymbol{v}}_{\mathrm{u}} \\ \mathbf{0} \end{pmatrix} - \begin{pmatrix} \boldsymbol{\Phi} & \mathbf{0} \\ \mathbf{0} & \mathbf{0} \end{pmatrix} (\mathbb{M}_{\mathrm{f}} + \bar{\mathbb{M}})\,\boldsymbol{\nu}_{\mathrm{r}} \end{aligned} \tag{13}$$

Comparing (13) with (10), we see that there is a term missing in Thomasson's equation, as discussed in Remark 2.2. To appreciate the role of this term, we follow an example presented in [7, Section III.B], an example that is also considered in [3, Art. 143]. Let the body be a neutrally buoyant sphere immersed in a steady, one-dimensional gradient flow. Suppose, without further loss of generality, that the flow speed is increasing in the inertial x direction. Noting that the added mass of a sphere is one-half of the displaced mass (m), the nontrivial component of equation (10) is

$$\frac{3}{2}m\dot{u} = \frac{3}{2}m\frac{du_{\mathrm{s}}}{dx}u - \frac{3}{2}m\frac{du_{\mathrm{s}}}{dx}(u - u_{\mathrm{s}}) + f_u$$

where f_u is the longitudinal component of the external force (e.g., drag, a constraint force, etc.). Simplifying a bit, we have

$$\dot{u} = \frac{du_{\mathrm{s}}}{dx}u_{\mathrm{s}} + \frac{2}{3}\frac{1}{m}f_u \tag{14}$$

In comparison, the nontrivial component of equation (13) gives

$$\dot{u} = -\frac{du_{\mathrm{s}}}{dx}(u - u_{\mathrm{s}}) + \frac{2}{3}\frac{1}{m}f_u \tag{15}$$

Lamb [3] and Thomasson [7] consider the special case in which the body is at rest: $u \equiv 0$. In this case, the two equations yield the same result: a force

$$m\frac{du_{\mathrm{s}}}{dx}u_{\mathrm{s}}$$

in the x direction due to the flow gradient. This result agrees with the example cited in [3]. (Note: There is a sign error in [7] when equation (54) is transcribed into equation (56).) If one considers the case where the body is free to move with the flow, however, equations (10) and (13) give different results.

Consider, for example, a case where the relative flow velocity is zero ($u = u_{\mathrm{s}} > 0$). In this case, equation (10) still results in a force due to the gradient, while equation (13) suggests that the force due to the gradient is zero. Intuitively, if a neutrally buoyant sphere is initially moving with the local flow velocity, it will accelerate with the flow and maintain zero relative velocity. (Consider that the rigid sphere in this example could be replaced by a ball of fluid.) This inertial acceleration is due to the ambient pressure force of the flow gradient.

Carrying the example a bit farther, suppose we write the dynamic equations in a flow-relative form, defining $u_{\mathrm{r}} = u - u_{\mathrm{s}}$. In the absence of other external forces, equation (14) gives

$$\dot{u}_{\mathrm{r}} = -\frac{du_{\mathrm{s}}}{dx}u_{\mathrm{r}}$$

while equation (15) gives

$$\dot{u}_{\mathrm{r}} = -\frac{du_{\mathrm{s}}}{dx}\left(2u_{\mathrm{r}} + u_{\mathrm{s}}\right)$$

The case $u_{\mathrm{r}} = 0$ is clearly an equilibrium for the former equation (a stable one, for a positive flow gradient). The latter equation has no such equilibrium, for any non-zero flow gradient. This example illustrates the importance of the term $\boldsymbol{\Phi v}$, as discussed in Remark 2.2.

2.4 Practical Extensions

Rotational flow. The principal application of the dynamic model presented above is for simulating the dynamics of a rigid body in a flow field. The chief limitation is that the flow is assumed to be irrotational. However, Thomasson suggests a minor modification to accommodate vorticity. Define an irrotational component $\boldsymbol{A} = \boldsymbol{A}^T$ and a rotational component $\hat{\boldsymbol{\omega}}_{\mathrm{f}}$ of the flow gradient matrix $|\boldsymbol{Phi}$ as follows:

$$\boldsymbol{\Phi} = \underbrace{\frac{1}{2}\left(\boldsymbol{\Phi} + \boldsymbol{\Phi}^T\right)}_{\boldsymbol{A}} + \frac{1}{2}\underbrace{\left(\boldsymbol{\Phi} - \boldsymbol{\Phi}^T\right)}_{-\hat{\boldsymbol{\omega}}_{\mathrm{f}}}$$

Thomasson suggests that one may incorporate the rotational component of the flow gradient

$$\boldsymbol{\omega}_{\mathrm{f}} = \begin{pmatrix} p_{\mathrm{f}} \\ q_{\mathrm{f}} \\ r_{\mathrm{f}} \end{pmatrix}$$

when computing viscous effects such as angular rate damping. What is not made clear in [7] is how to treat this asymmetric component in the equations previously derived. An underlying assumption of the derivation is that the flow is irrotational. If that is not the case, however, there is no physical rationale for simply omitting the asymmetric component $\hat{\boldsymbol{\omega}}_{\mathrm{f}}$ and proceeding. As a practical matter, one might simply retain the gradient (symmetric or otherwise) when computing ideal fluid effects, treating viscous effects such as damping moments due to the relative angular rate as described by Thomasson [7].

Slowly varying nonuniform flow. The development in Section 2 allows for *uniform* flow accelerations. In the case of a nonuniform unsteady flow, one might still employ the model presented here provided that the flow field varies slowly relative to the vehicle dynamic modes. Potential applications include planning of time- or energy-optimal paths. Slow variations can be captured in the flow field model using flow prediction software and/or using measurement data. For example, Petrich *et al.* [5] describe a method for identifying a simple, local flow model using navigation error measurements obtained by a collective of small underwater vehicles. The flow model employed in [5] comprises a uniform flow component and a component defined by a flow singularity (e.g., a source and/or a vortex) at some location. Though the paper considered only planar flow models, the method can be extended to three-dimensional flows.

3 Dynamics of a Vehicle with Symmetry

If we assume that $\boldsymbol{C}_{\mathrm{f}} = \boldsymbol{0}$ in the definition of $\mathbb{M}_{\mathrm{f}}$, then

$$\mathbb{M}_{\mathrm{f}} + \mathbb{M} = \begin{pmatrix} \boldsymbol{M} & -m\hat{\boldsymbol{r}}_{\mathrm{cm}} \\ m\hat{\boldsymbol{r}}_{\mathrm{cm}} & \boldsymbol{I} \end{pmatrix}$$

where

$$\boldsymbol{M} = m\mathbb{I} + \boldsymbol{M}_{\mathrm{f}} \qquad \text{and} \qquad \boldsymbol{I} = \boldsymbol{I}_{\mathrm{rb}} + \boldsymbol{I}_{\mathrm{f}}$$

Note that $\boldsymbol{C}_{\mathrm{f}}$ will generally be nonzero for a vehicle with tail fins; see Appendix C. It is common in AUV control design and analysis, however, to neglect this coupling in the added inertia matrix.

Assuming the vehicle is neutrally buoyant ($m = \bar{m}$), we have

$$\mathbb{M} - \bar{\mathbb{M}} = \begin{pmatrix} \mathbf{0} & -m\hat{\boldsymbol{r}}_{\rm cm} \\ m\hat{\boldsymbol{r}}_{\rm cm} & \boldsymbol{I}_{\rm rb} \end{pmatrix} \qquad \text{and} \qquad \mathbb{M}_{\rm f} + \bar{\mathbb{M}} = \begin{pmatrix} \boldsymbol{M} & \mathbf{0} \\ \mathbf{0} & \boldsymbol{I}_{\rm f} \end{pmatrix}$$

Substituting these expressions into equations (12), as described in Appendix B, gives

$$\begin{pmatrix} \boldsymbol{M} & -m\hat{\boldsymbol{r}}_{\rm cm} \\ m\hat{\boldsymbol{r}}_{\rm cm} & \boldsymbol{I} \end{pmatrix} \begin{pmatrix} \dot{\boldsymbol{v}}_{\rm r} \\ \dot{\boldsymbol{\omega}} \end{pmatrix} = \begin{pmatrix} (\boldsymbol{M}\boldsymbol{v}_{\rm r} - m\hat{\boldsymbol{r}}_{\rm cm}\boldsymbol{\omega}) \times \boldsymbol{\omega} - \boldsymbol{\Phi}\boldsymbol{M}\boldsymbol{v}_{\rm r} + \boldsymbol{f} \\ \boldsymbol{I}\boldsymbol{\omega} \times \boldsymbol{\omega} + \boldsymbol{M}\boldsymbol{v}_{\rm r} \times \boldsymbol{v}_{\rm r} - m\hat{\boldsymbol{r}}_{\rm cm}\left(\boldsymbol{\omega} \times \boldsymbol{v}_{\rm r} + \frac{\partial}{\partial t}\boldsymbol{v}_{\rm u} + \boldsymbol{\Phi}^T\boldsymbol{v}\right) + \boldsymbol{m} \end{pmatrix} \tag{16}$$

Notice that while the force $\boldsymbol{f}_\Phi = -\boldsymbol{\Phi}\boldsymbol{M}\boldsymbol{v}_{\rm r}$ scales with the relative velocity $\boldsymbol{v}_{\rm r}$, the moment $\boldsymbol{m}_\Phi = -m\hat{\boldsymbol{r}}_{\rm cm}\boldsymbol{\Phi}^T\boldsymbol{v}$ scales with the *absolute* velocity $\boldsymbol{v}$. Thus, a vehicle that is drifting in a strong flow ($\|\boldsymbol{v}\| \gg \|\boldsymbol{v}_{\rm r}\|$) may experience a significant disturbance moment $\boldsymbol{m}_\Phi$ due to a flow gradient even when the corresponding disturbance force $\boldsymbol{f}_\Phi$ is small due to a low relative velocity.

3.1 Dynamics of a Spherical Drifter

Lagrangian drifters are often used in ocean and atmospheric science to sample ambient properties and to measure large scale flows [9, Ch. 18]. For a spherical drifter, we model the viscous force as follows:

$$\boldsymbol{f}_{\rm v} = -\left(\frac{1}{2}\rho S C_D\right)|\boldsymbol{v}_{\rm r}|\boldsymbol{v}_{\rm r} \qquad \text{where} \qquad |\boldsymbol{v}_{\rm r}|\boldsymbol{v}_{\rm r} = \begin{pmatrix} |u_{\rm r}|u_{\rm r} \\ |v_{\rm r}|v_{\rm r} \\ |w_{\rm r}|w_{\rm r} \end{pmatrix}$$

The parameter ρ is the density, S is a characteristic area (e.g., the frontal area), and C_D is assumed to be constant.[1] For a spherical drifter, the viscous moment due to skin friction will be quite small and is assumed to be negligible.

The gravitational force and moment are

$$\boldsymbol{f}_{\rm g/b} = (m - \bar{m})g\boldsymbol{R}^T\boldsymbol{i}_3 \qquad \text{where} \qquad \boldsymbol{m}_{\rm g/b} = \boldsymbol{r}_{\rm cm} \times (mg\boldsymbol{R}^T\boldsymbol{i}_3)$$

Assuming that the drifter is neutrally buoyant, $\boldsymbol{f}_{\rm g/b} = \mathbf{0}$. With $\boldsymbol{r}_{\rm cm} \neq \mathbf{0}$, the gravitational moment will generate a preferred attitude for which the center of mass is directly below the center of buoyancy.

For a spherical drifter, $\boldsymbol{M}_{\rm f} = \frac{1}{2}m\mathbb{I}$ and $\boldsymbol{I}_{\rm f} = \mathbf{0}$. While these expressions lead to some simplifications, equations (16) still represent a coupled system of translational and rotational dynamic equations when $\boldsymbol{r}_{\rm cm} \neq \mathbf{0}$. In addition to inertial coupling, the term $\boldsymbol{r}_{\rm cm}$ introduces a moment due to the flow acceleration

$$-m\hat{\boldsymbol{r}}_{\rm cm}\left(\boldsymbol{\omega} \times \boldsymbol{v}_{\rm r} + \frac{\partial}{\partial t}\boldsymbol{v}_{\rm u} + \boldsymbol{\Phi}^T\boldsymbol{v}\right)$$

This term will have a significant effect on the dynamics, however, only when the magnitude of the terms in parenthesis is comparable to g. While such strong gradients may occur locally within a river or a tidal flow, drifters are typically deployed in more benign environments where one would not expect significant rotational motion due to flow gradient effects. Still, the equations suggest

[1] In incompressible flow, the drag coefficient C_D is determined by the geometry and the *Reynolds number*, Re. For a sphere, the value of C_D remains fairly constant provided $10^3 < \mathrm{Re} < 10^5$. See [10, pg. 182], for example.

that attitude perturbations due to the flow acceleration might be used to characterize the local flow field.

Suppose now that $\boldsymbol{r}_{\rm cm} = \boldsymbol{0}$. In this case, equations (16) decouple as follows:

$$m\dot{\boldsymbol{v}}_{\rm r} = m\boldsymbol{v}_{\rm r} \times \boldsymbol{\omega} - \left(\frac{1}{3}\rho S C_D\right)|\boldsymbol{v}_{\rm r}|\boldsymbol{v}_{\rm r} - m\boldsymbol{\Phi}\boldsymbol{v}_{\rm r} \tag{17}$$

$$\boldsymbol{I}_{\rm rb}\dot{\boldsymbol{\omega}} = (\boldsymbol{I}_{\rm rb}\boldsymbol{\omega}) \times \boldsymbol{\omega} \tag{18}$$

Equations (18) are well-known as Euler's equations for the free rotation of a rigid body. Equations (17) describe the drifter's translational dynamics. Flow gradients enter as a perturbation force, but one that is scaled by the relative velocity $\boldsymbol{v}_{\rm r}$ which remains small due to drag. One should therefore expect a Lagrangian drifter's path to closely match pathlines of the flow, suggesting that the commonly used "kinematic particle" model is appropriate in this case.

3.2 Dynamics and Control of an Underwater Vehicle

Consider a slender underwater vehicle, modeled as a prolate spheroid with a thruster and control planes. Suppose we fix a body reference frame in the spheroid principal axes such that the x-axis is the longitudinal axis. Explicit expressions for the added mass and inertia parameters defining the hull's contribution to $\mathbb{M}_f$ can be found in [3, Art. 114]. Added mass and inertia contributions due to appendages, such as control planes, can be computed as described in [4]. Details of the model are given in Appendix C.

Aside from the potential flow effects, as captured by the added mass and inertia, the external forces and moments acting on the body are those due to

- gravity and buoyancy ($\boldsymbol{f}_{\rm g/b}$ and $\boldsymbol{m}_{\rm g/b}$)
- viscous effects ($\boldsymbol{f}_{\rm v}$ and $\boldsymbol{m}_{\rm v}$), and
- propulsion and control ($\boldsymbol{f}_{\rm ctrl}$ and $\boldsymbol{m}_{\rm ctrl}$)

The complete external force and moment are

$$\begin{aligned} \boldsymbol{f} &= \boldsymbol{f}_{\rm g/b} + \boldsymbol{f}_{\rm v} + \boldsymbol{f}_{\rm ctrl} \\ \boldsymbol{m} &= \boldsymbol{m}_{\rm g/b} + \boldsymbol{m}_{\rm v} + \boldsymbol{m}_{\rm ctrl} \end{aligned}$$

Assuming that the body is neutrally buoyant ($m = \bar{m}$), the combined force $\boldsymbol{f}_{\rm g/b}$ due to gravity and buoyancy vanishes. If we let $\boldsymbol{r}_{\rm cm} = [0, 0, \gamma]^T$ with $\gamma > 0$, then gravity will provide a moment

$$\boldsymbol{m}_{\rm g/b} = \boldsymbol{r}_{\rm cm} \times mg\boldsymbol{R}^T\boldsymbol{i}_3$$

that provides stability in pitch and roll.

Viscous effects depend on the vehicle's flow-relative translational and rotational velocity. Recalling the discussion in Section 2.4 concerning the irrotational and rotational components of the flow field, we write

$$\boldsymbol{f}_{\rm v}(\boldsymbol{v}_{\rm r}, \boldsymbol{\omega}_{\rm r}) \quad \text{and} \quad \boldsymbol{m}_{\rm v}(\boldsymbol{v}_{\rm r}, \boldsymbol{\omega}_{\rm r})$$

where $\boldsymbol{\omega}_\mathrm{r} = \boldsymbol{\omega} - \boldsymbol{\omega}_\mathrm{f}$.

The control forces and moments are typically generated using external effectors (e.g., propulsors and control planes) which alter the viscous force and moment acting on the vehicle. We account for propulsion and control effects separately from viscous effects, through the control force $\boldsymbol{f}_\mathrm{ctrl}$ and the control moment $\boldsymbol{m}_\mathrm{ctrl}$.

3.2.1 Model Comparisons

This section compares results of numerical simulations of the given dynamic equations with simulations of simpler motion models. The autonomous underwater vehicle (AUV) model used for these simulations is described in Appendix C. The AUV hull is a prolate spheroid 2 meters long with a fineness ratio of 10:1. The four identical tail fins, arranged in a cruciform configuration, have an aspect ratio of 3; the tip-to-tip span for each pair of fins is 50 centimeters.

The vessel is trimmed to be neutrally buoyant and the thrust is fixed such that the nominal speed is $\tilde{u} > 0$. Vehicle attitude is regulated through proportional-derivative feedback.

In the first set of simulations, a steady, nonuniform flow is established by a point vortex (or rather a vertical line vortex) of strength 150 m^2/s located at the origin. The vortex results in a clockwise flow (as viewed from above) which diminishes with distance from the origin; the flow field is irrotational everywhere except at the origin. In the first simulation, the vehicle approaches from a point 80 m south and 20 m east of the point vortex, with an initial course that is due north. In the second simulation, the vehicle travels slower relative to the flow field, so the start point is chosen such that the flow has a weaker effect. The start point is 25 m south and 25 m east of the point vortex, again with an initial course that is due north.

Figures 3(a) and 3(b) show horizontal tracks for two nominal speeds ($u_\mathrm{d} = 5$ m/s and 2 m/s, respectively) corresponding to four scenarios:

1. Open-loop motion simulated using the full dynamic equations (12). (Solid blue curve)
2. Open-loop motion simulated using a simplified mode: the first line of equations (12). (Dashed blue curve)
3. Closed-loop motion simulated using the full dynamic equations with a $\pm 5^\circ$ square wave heading reference.[2] (Solid red curve)
4. Closed-loop motion simulated using the simplified model with a square wave heading reference. (Dashed red curve)

For the faster nominal speed ($u_\mathrm{d} = 5$ m/s), the open-loop trajectories compare well with one another, as do the close-loop trajectories, despite the omitted gradient effects in the simpler model. A small disturbance in the heading angle ψ is visible in the solid (full model) traces in Figure 4(c) at around 20 seconds, indicating that the vortex induces an appreciable moment when the vehicle nears the vortex center. A corresponding excursion in relative sideslip angle $\beta_\mathrm{r} \approx v_\mathrm{r}/u_\mathrm{d}$ is visible in Figure 4(d). In general, however, the agreement between the simplified and full dynamic model is quite good for this case where the vehicle is traveling relatively fast.

[2] In applications where inertial velocity measurements are available, it may be more appropriate to regulate course angle rather than heading angle. For AUVs, however, inertial velocity measurements are typically unavailable.

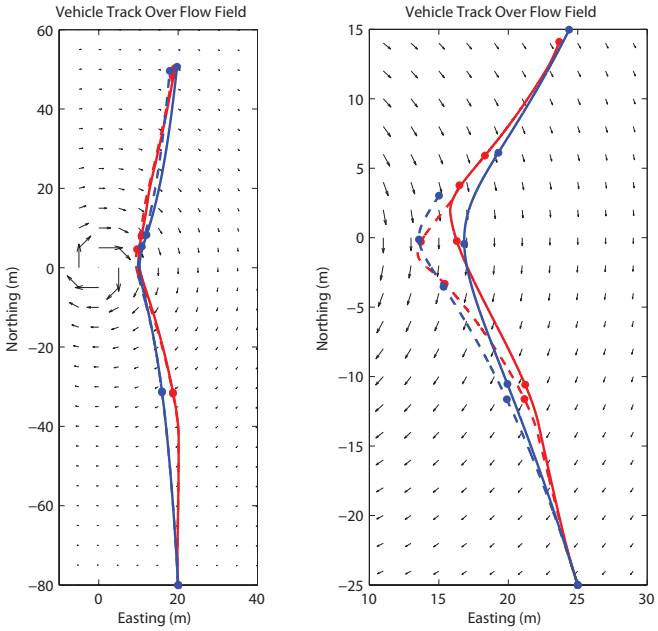

(a) $u_d = 5$ m/s (b) $u_d = 2$ m/s

Figure 3: Comparison of full and simplified rigid body dynamic model simulations with open- and closed-loop control in a vortical flow field. Simulation cases are open-loop full dynamic model (solid blue), open-loop simplified dynamic model (dashed blue), closed-loop full dynamic model (solid red), and closed-loop simplified dynamic model (dashed red). Dots indicate 10 second intervals.

For the slower nominal speed ($u_d = 2$ m/s), there is greater discrepancy between the full and simplified models. Even though the vehicle trajectory passes farther from the vortex center, the effect of the flow gradient on the vehicle path is more significant. Notice that the relative sideslip angle β_r in Figure 5(d) returns to zero for the full dynamic model after each heading change, as it does for the simplified model. That a vehicle traveling at a lower flow-relative speed may be more subject to flow gradients has implications for the stabilization and control of weakly propelled vehicles in significant currents, such as underwater gliders operating in coastal waters.

In a second set of simulations, the vehicle travels north in a steady, nonuniform flow field comprising a uniform 35 cm/s southward flow and an eastward component that varies sinusoidally with northward position; the amplitude is 35 cm/s and the wavelength is 100 m. Note that this flow field is not irrotational; in the simulations, rotational flow components contribute to an effective angular rate which affects the angular rate damping moment.

Figures 6(a) and 6(b) show time-stamped horizontal paths that result under four scenarios when $u_d = 5$ m/s and 1 m/s, respectively:

1. Open-loop motion simulated using the full dynamic equations (12). (Solid blue curve)
2. Open-loop motion simulated using the "kinematic particle model" in which the vehicle velocity is simply the sum of the commanded flow-relative velocity and the flow velocity. (Dashed blue curve)
3. Closed-loop motion simulated using the full dynamic equations with a $\pm 15^\circ$ square wave

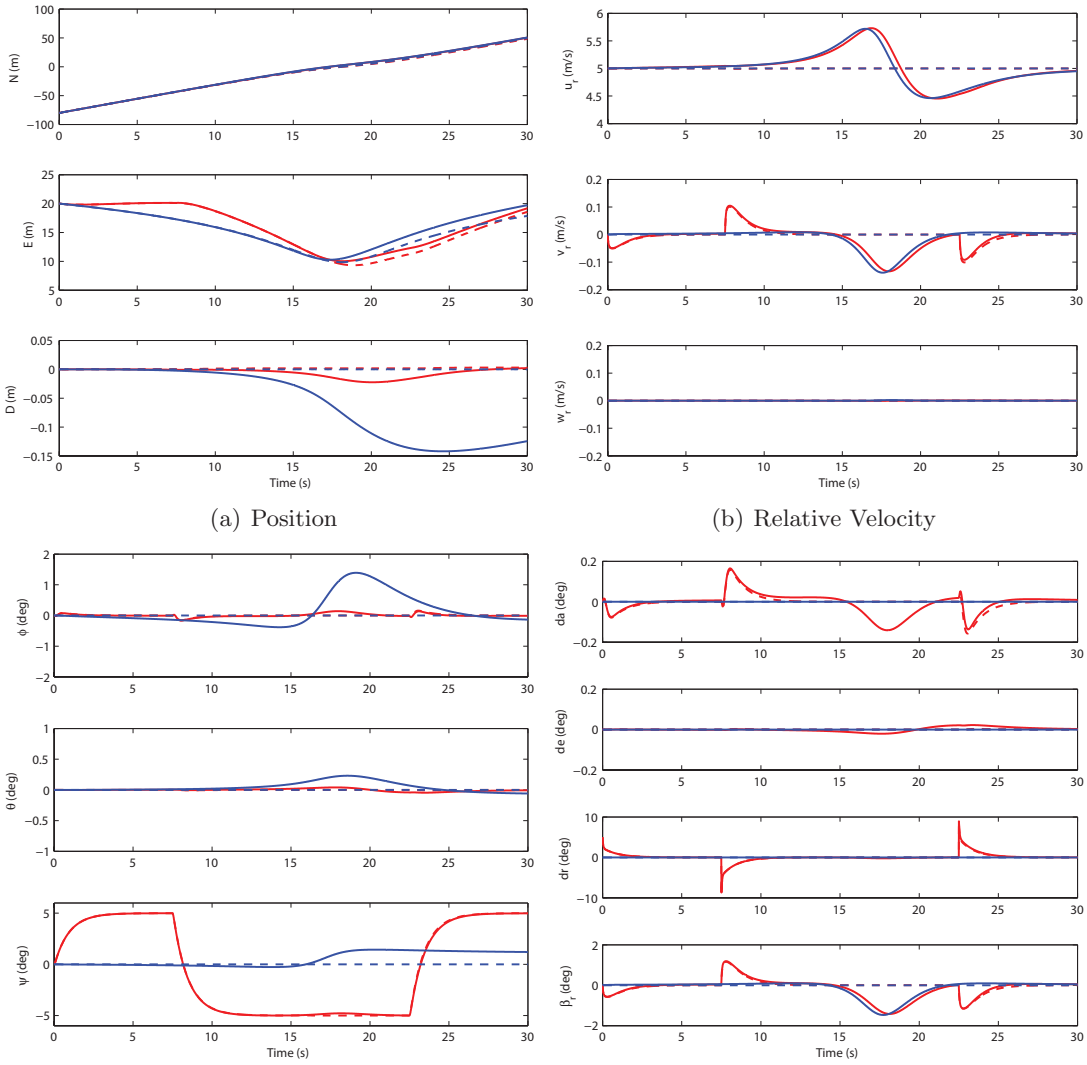

(a) Position

(b) Relative Velocity

(c) Attitude

(d) Inputs and Sideslip

Figure 4: Comparison of full and simplified rigid body dynamic model simulations with open- and closed-loop control in a vortical flow field. Simulation cases are open-loop full dynamic model (solid blue), open-loop simplified dynamic model (dashed blue), closed-loop full dynamic model (solid red), and closed-loop simplified dynamic model (dashed red).

heading reference. (Solid red curve)

4. Closed-loop motion simulated using the kinematic particle model. (Dashed red curve)

Under closed-loop control, the vehicle path for the kinematic model remains close to that of the full dynamic model, but the turning dynamics introduce a noticeable lag in the path for the dynamic model. In the open-loop case, there is a noticeable discrepancy between the kinematic and full dynamic model. Recall, for the kinematic model, that the vehicle velocity is simply the vector sum of the commanded velocity (due north) and the flow field velocity while, for the dynamic model, the flow gradient induces turning moments on the vehicle. In the open-loop simulation, the turning moment is such that the vehicle noses away from the flow, increasing the vehicle's lateral excursion;

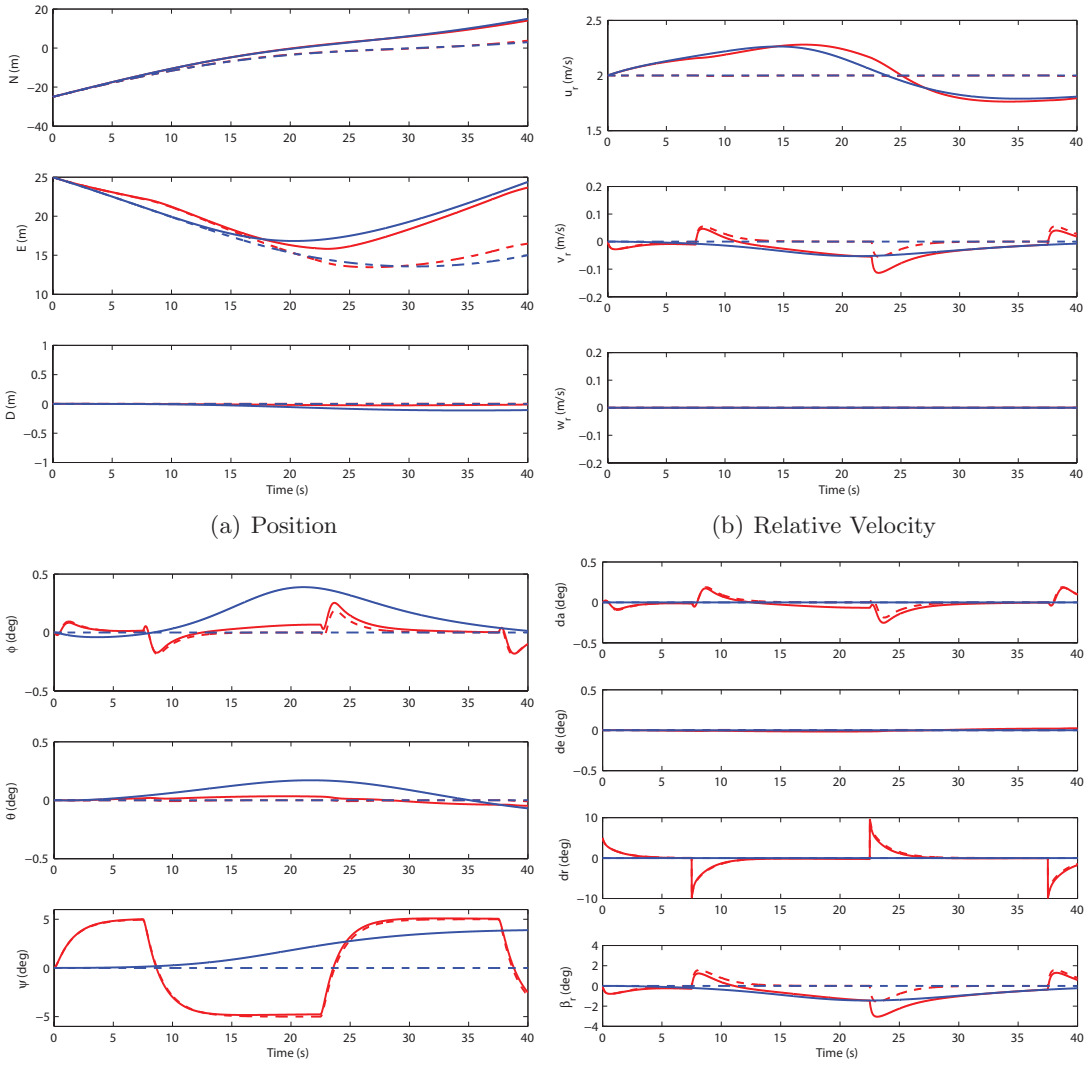

(a) Position

(b) Relative Velocity

(c) Attitude

(d) Inputs and Sideslip

Figure 5: Comparison of full and simplified rigid body dynamic model simulations with open- and closed-loop control in a vortical flow field. Simulation cases are open-loop full dynamic model (solid blue), open-loop simplified dynamic model (dashed blue), closed-loop full dynamic model (solid red), and closed-loop simplified dynamic model (dashed red).

see Figure 6(b).

3.2.2 Local Analysis

Assume, for the moment, that there is no flow acceleration (i.e., no gradients or unsteadiness). With conventional assumptions concerning symmetry of the vehicle, a constant propulsive force acting along the surge axis results in a steady motion of the form

$$\tilde{\boldsymbol{v}}_{\mathrm{r}} = \begin{pmatrix} \tilde{u}_{\mathrm{r}} \\ 0 \\ 0 \end{pmatrix} \qquad \text{and} \qquad \tilde{\boldsymbol{\omega}} = \boldsymbol{0}$$

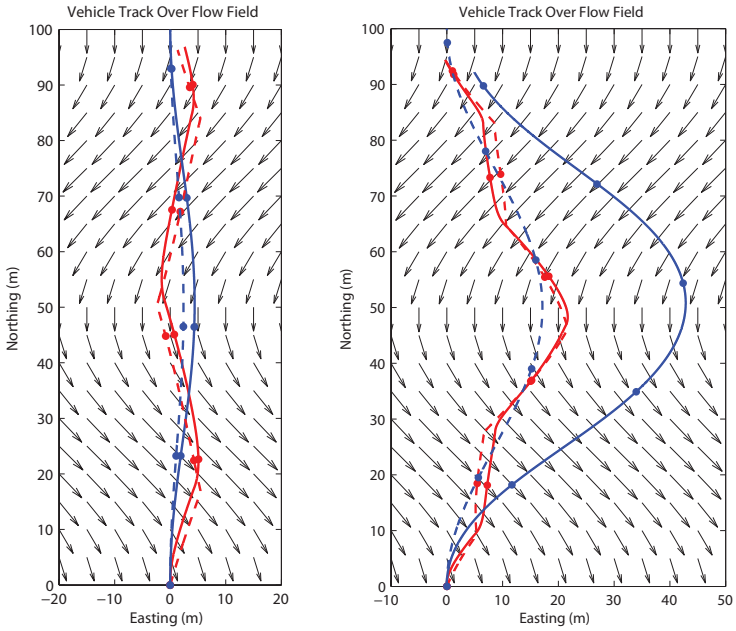

(a) $u_{\mathrm{d}} = 5$ m/s. (b) $u_{\mathrm{d}} = 1$ m/s.

Figure 6: Comparison of rigid body dynamic and kinematic particle model simulations with open- and closed-loop control in a sinusoidal flow field with two different nominal relative speeds u_{d}. Simulation cases are open-loop rigid body dynamic model (solid blue), open-loop kinematic particle model (dashed blue), closed-loop rigid body dynamic model (solid red), and closed-loop kinematic particle model (dashed red). Dots indicate 5 second intervals for the higher speed and 30 second intervals for the lower.

In this condition, thrust is balanced drag ($\boldsymbol{f}_{\mathrm{v}} + \boldsymbol{f}_{\mathrm{ctrl}} = \boldsymbol{0}$) and no control moment is required to maintain the steady motion ($\boldsymbol{m}_{\mathrm{ctrl}} = \boldsymbol{0}$). Determining the *stability* of the steady motion requires analyzing the vehicle's response to small perturbations. Linearizing about the steady motion above yields the small perturbation equations

$$\begin{pmatrix} \boldsymbol{M} & -m\hat{\boldsymbol{r}}_{\mathrm{cm}} \\ m\hat{\boldsymbol{r}}_{\mathrm{cm}} & \boldsymbol{I} \end{pmatrix} \begin{pmatrix} \Delta\dot{\boldsymbol{v}}_{\mathrm{r}} \\ \Delta\dot{\boldsymbol{\omega}} \end{pmatrix} = \begin{pmatrix} \boldsymbol{0} & \widehat{\boldsymbol{M}\tilde{\boldsymbol{v}}}_{\mathrm{r}} \\ \left(\widehat{\boldsymbol{M}\tilde{\boldsymbol{v}}}_{\mathrm{r}} - \hat{\tilde{\boldsymbol{v}}}_{\mathrm{r}}\boldsymbol{M}\right) & m\hat{\boldsymbol{r}}_{\mathrm{cm}}\hat{\tilde{\boldsymbol{v}}}_{\mathrm{r}} \end{pmatrix} \begin{pmatrix} \Delta\boldsymbol{v}_{\mathrm{r}} \\ \Delta\boldsymbol{\omega} \end{pmatrix} + \begin{pmatrix} \Delta\boldsymbol{f} \\ \Delta\boldsymbol{m} \end{pmatrix}$$

where $\Delta\boldsymbol{v}_{\mathrm{r}} = \boldsymbol{v}_{\mathrm{r}} - \tilde{\boldsymbol{v}}_{\mathrm{r}}$ and $\Delta\boldsymbol{\omega} = \boldsymbol{\omega} - \tilde{\boldsymbol{\omega}}$. If the vehicle then encounters a nonuniform flow field, the effect changes the flow-relative translational and rotational velocity and adds the forcing term:

$$-\begin{pmatrix} \boldsymbol{\Phi}\boldsymbol{M}\boldsymbol{v}_{\mathrm{r}} \\ m\hat{\boldsymbol{r}}_{\mathrm{cm}}\left((\boldsymbol{v}_{\mathrm{u}} + \boldsymbol{v}_{\mathrm{s}}) \times \boldsymbol{\omega} + \frac{\partial}{\partial t}\boldsymbol{v}_{\mathrm{u}} + \boldsymbol{\Phi}^{T}\boldsymbol{v}\right) \end{pmatrix}$$

For illustrative purposes, we focus on the dynamics of an underwater vehicle moving in the horizontal plane. The horizontal plane components of the linearized dynamics equations for a vehicle

with a conventional thrust (δT) and rudder (δr) model are

$$\begin{pmatrix} m_x \Delta\dot{u}_{\mathrm{r}} \\ m_y \Delta\dot{v}_{\mathrm{r}} \\ I_{zz}\Delta\dot{r} \end{pmatrix} = \begin{pmatrix} \tilde{X}_u & 0 & 0 \\ 0 & Y_v & Y_r - m_x\tilde{u}_{\mathrm{r}} \\ 0 & N_v + (m_x - m_y)\tilde{u}_{\mathrm{r}} & N_r \end{pmatrix} \begin{pmatrix} \Delta u_{\mathrm{r}} \\ \Delta v_{\mathrm{r}} \\ \Delta r \end{pmatrix} - \begin{pmatrix} 0 \\ Y_r \\ N_r \end{pmatrix} r_{\mathrm{f}}$$
$$- \begin{pmatrix} \begin{pmatrix} \cos\tilde{\psi} & \sin\tilde{\psi} \\ -\sin\tilde{\psi} & \cos\tilde{\psi} \end{pmatrix} \begin{pmatrix} \frac{\partial V_{\mathrm{f}_\xi}}{\partial \xi} & \frac{\partial V_{\mathrm{f}_\xi}}{\partial \eta} \\ \frac{\partial V_{\mathrm{f}_\eta}}{\partial \xi} & \frac{\partial V_{\mathrm{f}_\eta}}{\partial \eta} \end{pmatrix}^T \begin{pmatrix} \cos\tilde{\psi} & -\sin\tilde{\psi} \\ \sin\tilde{\psi} & \cos\tilde{\psi} \end{pmatrix} \begin{pmatrix} m_x(\tilde{u}_{\mathrm{r}} + \Delta u_{\mathrm{r}}) \\ m_y \Delta v_{\mathrm{r}} \end{pmatrix} \\ 0 \end{pmatrix}$$
$$+ \begin{pmatrix} X_{\delta T} & 0 \\ 0 & Y_{\delta r} \\ 0 & N_{\delta r} \end{pmatrix} \begin{pmatrix} \delta T \\ \delta r \end{pmatrix} \tag{19}$$

where $\tilde{X}_u$, $Y_{(\cdot)}$, and $N_{(\cdot)}$ represent force and moment sensitivities to the indicated variables.[3] Recall from Section 2.4 that the term r_{f} accounts for an effective yaw angular rate due to the flow gradient which affects the viscous force and moment terms.

For a well-designed vehicle, the 3×3 state matrix appearing in the first line of (19) is Hurwitz so that that the nominal motion is asymptotically stable. The effect of the flow gradient is a disturbance force which perturbs the vehicle from its nominal state of motion.

As an example, suppose that the vessel maintains a *northerly* heading ($\tilde{\psi} = 0$) in a planar flow whose easterly component varies sinusoidally with northward position:

$$\boldsymbol{V}_{\mathrm{f}}(\boldsymbol{X}) = \begin{pmatrix} V_{\mathrm{f}_\xi} \\ V_{\mathrm{f}_\eta} \\ V_{\mathrm{f}_\zeta} \end{pmatrix} = \begin{pmatrix} \bar{V}_{\mathrm{f}_\xi} \\ V_{\mathrm{f}_\eta}(\xi) \\ 0 \end{pmatrix}$$

The northward flow component $\bar{V}_{\mathrm{f}_\xi}$ is constant.

We assume that the yaw angle remains small: $\psi \approx \tilde{\psi} = 0$. We also assume that the flow gradient

$$\frac{\partial V_{\mathrm{f}_\eta}}{\partial \xi}$$

is small, so that products with perturbation variables may be ignored. Neglecting higher order terms in the perturbation variables, the surge dynamics decouple from the steering dynamics:

$$m_x \Delta\dot{u}_{\mathrm{r}} = \tilde{X}_u \Delta u_{\mathrm{r}} + X_{\delta T}\delta T$$

and

$$\begin{pmatrix} m_y \Delta\dot{v}_{\mathrm{r}} \\ I_{zz}\Delta\dot{r} \end{pmatrix} = \begin{pmatrix} Y_v & Y_r - m_x\tilde{u}_{\mathrm{r}} \\ N_v + (m_x - m_y)\tilde{u}_{\mathrm{r}} & N_r \end{pmatrix} \begin{pmatrix} \Delta v_{\mathrm{r}} \\ \Delta r \end{pmatrix}$$
$$- \begin{pmatrix} Y_r + m_x\tilde{u}_{\mathrm{r}} \\ N_r \end{pmatrix} \left(\frac{\partial V_{\mathrm{f}_\eta}}{\partial \xi} \right) + \begin{pmatrix} Y_{\delta r} \\ N_{\delta r} \end{pmatrix} \delta r \tag{20}$$

Note that the lateral force is proportional to the product of the flow gradient and the flow-relative vehicle speed. For low flow-relative speeds and small gradients, the effect of the disturbance vanishes. For higher speeds and/or larger gradients the effect can be significant.

[3] The term $\tilde{X}_u = X_u + 2X_{|u|u}\tilde{u}_{\mathrm{r}}$ includes a component that accounts for quadratic drag when $\tilde{u}_{\mathrm{r}} \neq 0$. The over-tilde distinguishes the damping parameter $\tilde{X}_u$ from the zero-velocity parameter X_u.

For a well-designed vehicle, the steering dynamics in the system (20) are stable and act as a *low-pass filter* for the disturbance due to the flow gradient. Thus, if the frequency content of the disturbance term

$$-\begin{pmatrix} Y_r + m_x \tilde{u}_{\mathrm{r}} \\ N_r \end{pmatrix} \left(\frac{\partial V_{\mathrm{f}_\eta}}{\partial \xi} \right) \tag{21}$$

is much higher than the natural frequency of the steering dynamics (20), the disturbance will be filtered by the vehicle's natural dynamics and the flow field's effect on the vehicle dynamics can simply be ignored. If the frequency content of the disturbance (21) is below or commensurate with the natural frequency of the system, however, the disturbance will be passed into the vehicle's motion resulting in nonzero sideslip and turn rate perturbations. Suppose, for example, that a lateral flow varies sinusoidally in the northward direction with wavelength λ and amplitude A:

$$V_{\mathrm{f}_\eta}(\xi) = A \sin\left(\frac{2\pi\xi}{\lambda} \right)$$

In this case,

$$\frac{\partial V_{\mathrm{f}_\eta}}{\partial \xi} = A \left(\frac{2\pi}{\lambda} \right) \cos\left(\frac{2\pi\xi}{\lambda} \right)$$

Since $\dot{\xi}(t) \approx \tilde{u}$, the flow gradient will impose a periodic lateral force with frequency $\frac{2\pi\tilde{u}}{\lambda}$. Because the vessel acts as a low-pass filter, forcing at shorter wavelengths λ and higher speeds $\tilde{u}$ will be attenuated, even though the amplitude scales inversely with the wavelength. Forcing at longer wavelengths and lower speeds, however, may have an appreciable effect on the steering dynamics.

4 Conclusions

Following up on the work of Thomasson [7], the dynamic equations are derived for a rigid vehicle that is moving in a dense, moving fluid. The fluid motion is assumed to be irrotational and is defined as the sum of a steady, circulating component and an unsteady, uniform component. Rotational flow effects can be incorporated by appropriately modifying the vehicle angular rate when computing viscous forces and moments. Some errors in Thomasson's original paper are identified and corrected and the equations are presented in a format more familiar to the marine vehicle dynamics community. Applications of these dynamic equations include:

- Motion prediction and control validation for unmanned surface and underwater vehicles operating in significant currents.
- Motion prediction and control validation for weakly actuated riverine drifters.
- Design and assessment of energy harvesting devices operating in flow gradients.

Acknowledgments. The author is very grateful to Pete Thomasson for his encouragement and for a very fruitful discussion concerning vehicle motion in dense, moving fluids. The analysis presented here was sponsored in part by ONR Grants Nos. N00014-08-1-0012 and N00014-10-1-0185.

References

[1] B. Etkin. *Dynamics of Atmospheric Flight*. John Wiley and Sons, 1972.

[2] T. I. Fossen. *Guidance and Control of Ocean Vehicles*. John Wiley and Sons, 1995.

[3] H. Lamb. *Hydrodynamics*. Dover, New York, NY, 1945.

[4] E. M. Lewandowski. *The Dynamics of Marine Craft*. World Scientific, River Edge, NJ, 2004.

[5] J. Petrich, C. A. Woolsey, and D. J. Stilwell. Planar flow model identification for improved navigation of small AUVs. *Ocean Engineering*, 36:119–131, November 2009.

[6] H. Schaub and J. L. Junkins. *Analytical Mechanics of Space Systems*. AIAA Education Series, Reston, VA, 2003.

[7] P. G. Thomasson. Equations of motion of a vehicle in a moving fluid. *Journal of Aircraft*, 37(4):630–639, 2000.

[8] P. G. Thomasson. On calculating the motion of a vehicle in a moving fluid. In *Proc. Third International Conf. on Non-Linear Problems in Aviation and Aerospace*, Daytona Beach, FL, 2000. European Conference Publications. (ISBN 0952-6643-2-1).

[9] C. Tropea, A. L. Yarin, and J. F. Foss. *Springer Handbook of Experimental Fluid Mechanics*. Springer-Verlag, 2007.

[10] F. M. White. *Viscous Fluid Flow*. McGraw-Hill, Inc., second edition, 1991.

A Derivation of Equation (12)

Here, we show that equation (12) follows from equation (11). In particular, we show that

$$
\begin{aligned}
&-\begin{pmatrix} \hat{\boldsymbol{\omega}} & \mathbf{0} \\ \hat{\boldsymbol{v}}_{\mathrm{r}} & \hat{\boldsymbol{\omega}} \end{pmatrix} \left(\mathbb{M}_{\mathrm{f}} + \bar{\mathbb{M}}\right) \boldsymbol{\nu}_{\mathrm{r}} - \begin{pmatrix} \hat{\boldsymbol{\omega}} & \mathbf{0} \\ \hat{\boldsymbol{v}} & \hat{\boldsymbol{\omega}} \end{pmatrix} \left(\mathbb{M} - \bar{\mathbb{M}}\right) \boldsymbol{\nu} \\
&\quad = \left[-\begin{pmatrix} \hat{\boldsymbol{\omega}} & \mathbf{0} \\ \hat{\boldsymbol{v}}_{\mathrm{r}} & \hat{\boldsymbol{\omega}} \end{pmatrix} \left(\mathbb{M}_{\mathrm{f}} + \mathbb{M}\right) \boldsymbol{\nu}_{\mathrm{r}} - \begin{pmatrix} \hat{\boldsymbol{\omega}} & \mathbf{0} \\ \hat{\boldsymbol{v}}_{\mathrm{r}} & \hat{\boldsymbol{\omega}} \end{pmatrix} \left(\bar{\mathbb{M}} - \mathbb{M}\right) \boldsymbol{\nu}_{\mathrm{r}}\right] \\
&\qquad + \left[-\begin{pmatrix} \hat{\boldsymbol{\omega}} & \mathbf{0} \\ \hat{\boldsymbol{v}} & \hat{\boldsymbol{\omega}} \end{pmatrix} \left(\mathbb{M} - \bar{\mathbb{M}}\right) \begin{pmatrix} \boldsymbol{v}_{\mathrm{u}} + \boldsymbol{v}_{\mathrm{s}} \\ \mathbf{0} \end{pmatrix} - \begin{pmatrix} \hat{\boldsymbol{\omega}} & \mathbf{0} \\ \hat{\boldsymbol{v}} & \hat{\boldsymbol{\omega}} \end{pmatrix} \left(\mathbb{M} - \bar{\mathbb{M}}\right) \boldsymbol{\nu}_{\mathrm{r}}\right] \\
&\quad = -\begin{pmatrix} \hat{\boldsymbol{\omega}} & \mathbf{0} \\ \hat{\boldsymbol{v}}_{\mathrm{r}} & \hat{\boldsymbol{\omega}} \end{pmatrix} \left(\mathbb{M}_{\mathrm{f}} + \mathbb{M}\right) \boldsymbol{\nu}_{\mathrm{r}} - \begin{pmatrix} \hat{\boldsymbol{\omega}} & \mathbf{0} \\ \hat{\boldsymbol{v}} & \hat{\boldsymbol{\omega}} \end{pmatrix} \left(\mathbb{M} - \bar{\mathbb{M}}\right) \begin{pmatrix} \boldsymbol{v}_{\mathrm{u}} + \boldsymbol{v}_{\mathrm{s}} \\ \mathbf{0} \end{pmatrix} \\
&\qquad - \begin{pmatrix} \mathbf{0} & \mathbf{0} \\ \hat{\boldsymbol{v}}_{\mathrm{u}} + \hat{\boldsymbol{v}}_{\mathrm{s}} & \mathbf{0} \end{pmatrix} \left(\mathbb{M} - \bar{\mathbb{M}}\right) \boldsymbol{\nu}_{\mathrm{r}}
\end{aligned} \tag{22}
$$

The claim follows immediately.

B Derivation of Equation (16)

Recall equation (12)

$$
\begin{aligned}
\left(\mathbb{M}_{\mathrm{f}} + \mathbb{M}\right) \dot{\boldsymbol{\nu}}_{\mathrm{r}} \;=\; & -\begin{pmatrix} \hat{\boldsymbol{\omega}} & \mathbf{0} \\ \hat{\boldsymbol{v}}_{\mathrm{r}} & \hat{\boldsymbol{\omega}} \end{pmatrix} \left(\mathbb{M}_{\mathrm{f}} + \mathbb{M}\right) \boldsymbol{\nu}_{\mathrm{r}} + \begin{pmatrix} \boldsymbol{f} \\ \boldsymbol{m} \end{pmatrix} \\
& - \begin{pmatrix} \hat{\boldsymbol{\omega}} & \mathbf{0} \\ \hat{\boldsymbol{v}} & \hat{\boldsymbol{\omega}} \end{pmatrix} \left(\mathbb{M} - \bar{\mathbb{M}}\right) \begin{pmatrix} \boldsymbol{v}_{\mathrm{u}} + \boldsymbol{v}_{\mathrm{s}} \\ \mathbf{0} \end{pmatrix} - \begin{pmatrix} \mathbf{0} & \mathbf{0} \\ \hat{\boldsymbol{v}}_{\mathrm{u}} + \hat{\boldsymbol{v}}_{\mathrm{s}} & \mathbf{0} \end{pmatrix} \left(\mathbb{M} - \bar{\mathbb{M}}\right) \boldsymbol{\nu}_{\mathrm{r}} \\
& - \left(\mathbb{M} - \bar{\mathbb{M}}\right) \begin{pmatrix} \left(\boldsymbol{v}_{\mathrm{u}} + \boldsymbol{v}_{\mathrm{s}}\right) \times \boldsymbol{\omega} + \frac{\partial}{\partial t} \boldsymbol{v}_{\mathrm{u}} + \boldsymbol{\Phi}^T \boldsymbol{v} \\ \mathbf{0} \end{pmatrix} - \begin{pmatrix} \boldsymbol{\Phi} & \mathbf{0} \\ \mathbf{0} & \mathbf{0} \end{pmatrix} \left(\mathbb{M}_{\mathrm{f}} + \bar{\mathbb{M}}\right) \boldsymbol{\nu}_{\mathrm{r}}
\end{aligned}
$$

With the specific expressions for the generalized inertia matrices given in Section 3, we obtain the flow-relative translational dynamics

$$
\boldsymbol{M} \dot{\boldsymbol{v}}_{\mathrm{r}} - m \hat{\boldsymbol{r}}_{\mathrm{cm}} \dot{\boldsymbol{\omega}} = -\boldsymbol{\omega} \times \left(\boldsymbol{M} \boldsymbol{v}_{\mathrm{r}} - m \hat{\boldsymbol{r}}_{\mathrm{cm}} \boldsymbol{\omega}\right) + \boldsymbol{f} - \boldsymbol{\Phi} \boldsymbol{M} \boldsymbol{v}_{\mathrm{r}} \tag{23}
$$

The flow-relative rotational dynamics are

$$
\begin{aligned}
\boldsymbol{I} \dot{\boldsymbol{\omega}} + m \hat{\boldsymbol{r}}_{\mathrm{cm}} \dot{\boldsymbol{v}}_{\mathrm{r}} \;=\; & -\boldsymbol{v}_{\mathrm{r}} \times \left(\boldsymbol{M} \boldsymbol{v}_{\mathrm{r}} - m \hat{\boldsymbol{r}}_{\mathrm{cm}} \boldsymbol{\omega}\right) - \boldsymbol{\omega} \times \left(\boldsymbol{I} \boldsymbol{\omega} + m \hat{\boldsymbol{r}}_{\mathrm{cm}} \boldsymbol{v}_{\mathrm{r}}\right) + \boldsymbol{m} \\
& -\boldsymbol{\omega} \times m \hat{\boldsymbol{r}}_{\mathrm{cm}} \left(\boldsymbol{v}_{\mathrm{u}} + \boldsymbol{v}_{\mathrm{s}}\right) - \left(\boldsymbol{v}_{\mathrm{u}} + \boldsymbol{v}_{\mathrm{s}}\right) \times \left(-m \hat{\boldsymbol{r}}_{\mathrm{cm}} \boldsymbol{\omega}\right) \\
& -m \boldsymbol{r}_{\mathrm{cm}} \times \left(\left(\boldsymbol{v}_{\mathrm{u}} + \boldsymbol{v}_{\mathrm{s}}\right) \times \boldsymbol{\omega} + \frac{\partial}{\partial t} \boldsymbol{v}_{\mathrm{u}} + \boldsymbol{\Phi}^T \boldsymbol{v}\right)
\end{aligned}
$$

On the second line, we may replace

$$
-\boldsymbol{\omega} \times m \hat{\boldsymbol{r}}_{\mathrm{cm}} \left(\boldsymbol{v}_{\mathrm{u}} + \boldsymbol{v}_{\mathrm{s}}\right) - \left(\boldsymbol{v}_{\mathrm{u}} + \boldsymbol{v}_{\mathrm{s}}\right) \times \left(-m \hat{\boldsymbol{r}}_{\mathrm{cm}} \boldsymbol{\omega}\right) = m \boldsymbol{r}_{\mathrm{cm}} \times \left(\left(\boldsymbol{v}_{\mathrm{u}} + \boldsymbol{v}_{\mathrm{s}}\right) \times \boldsymbol{\omega}\right)
$$

Similarly, in the first line we may replace

$$
\boldsymbol{v}_{\mathrm{r}} \times \left(m \boldsymbol{r}_{\mathrm{cm}} \times \boldsymbol{\omega}\right) + \boldsymbol{\omega} \times \left(\boldsymbol{v}_{\mathrm{r}} \times m \boldsymbol{r}_{\mathrm{cm}}\right) = -m \boldsymbol{r}_{\mathrm{cm}} \times \left(\boldsymbol{\omega} \times \boldsymbol{v}_{\mathrm{r}}\right)
$$

Summing the two contributions gives

$$-m\boldsymbol{r}_{\rm cm}\times(\boldsymbol{\omega}\times\boldsymbol{v})$$

so that

$$\begin{aligned}\boldsymbol{I}\dot{\boldsymbol{\omega}}+m\hat{\boldsymbol{r}}_{\rm cm}\dot{\boldsymbol{v}}_{\rm r} &= -\boldsymbol{v}_{\rm r}\times(\boldsymbol{M}\boldsymbol{v}_{\rm r})-\boldsymbol{\omega}\times(\boldsymbol{I}\boldsymbol{\omega})+\boldsymbol{m}\\ &\quad -m\hat{\boldsymbol{r}}_{\rm cm}\left(\boldsymbol{\omega}\times\boldsymbol{v}+(\boldsymbol{v}_{\rm u}+\boldsymbol{v}_{\rm s})\times\boldsymbol{\omega}+\frac{\partial}{\partial t}\boldsymbol{v}_{\rm u}+\boldsymbol{\Phi}^T\boldsymbol{v}\right)\\ &= -\boldsymbol{v}_{\rm r}\times(\boldsymbol{M}\boldsymbol{v}_{\rm r})-\boldsymbol{\omega}\times(\boldsymbol{I}\boldsymbol{\omega})+\boldsymbol{m}-m\hat{\boldsymbol{r}}_{\rm cm}\left(\boldsymbol{\omega}\times\boldsymbol{v}_{\rm r}+\frac{\partial}{\partial t}\boldsymbol{v}_{\rm u}+\boldsymbol{\Phi}^T\boldsymbol{v}\right) \quad (24)\end{aligned}$$

Equations (23) and (24) together give (16).

C Dynamic Model for a Spheroidal AUV

We consider a rigid, spheroidal vehicle that is neutrally buoyant ($m=\bar{m}$). The vehicle's tail section includes four stabilizer/control planes arranged in a cruciform configuration. The generalized added inertia matrix is

$$\mathbb{M}_{\rm f}=\begin{pmatrix}\boldsymbol{M}_{\rm f} & \boldsymbol{C}_{\rm f}\\ \boldsymbol{C}_{\rm f}^T & \boldsymbol{I}_{\rm f}\end{pmatrix}$$

Recalling that

$$\mathbb{M}=\begin{pmatrix}m\mathbb{I} & -m\hat{\boldsymbol{r}}_{\rm cm}\\ m\hat{\boldsymbol{r}}_{\rm cm} & \boldsymbol{I}_{\rm rb}\end{pmatrix}$$

we have

$$\mathbb{M}_{\rm f}+\mathbb{M}=\begin{pmatrix}\boldsymbol{M} & \boldsymbol{C}\\ \boldsymbol{C}^T & \boldsymbol{I}\end{pmatrix}$$

where

$$\boldsymbol{M}=m\mathbb{I}+\boldsymbol{M}_{\rm f},\qquad \boldsymbol{C}=\boldsymbol{C}_{\rm f}-m\hat{\boldsymbol{r}}_{\rm cm},\qquad \text{and}\qquad \boldsymbol{I}=\boldsymbol{I}_{\rm rb}+\boldsymbol{I}_{\rm f}$$

Also,

$$\mathbb{M}-\bar{\mathbb{M}}=\begin{pmatrix}\boldsymbol{0} & -m\hat{\boldsymbol{r}}_{\rm cm}\\ m\hat{\boldsymbol{r}}_{\rm cm} & \boldsymbol{I}_{\rm rb}\end{pmatrix}$$

and

$$\mathbb{M}_{\rm f}+\bar{\mathbb{M}}=\begin{pmatrix}\boldsymbol{M} & \boldsymbol{C}_{\rm f}\\ \boldsymbol{C}_{\rm f}^T & \boldsymbol{I}_{\rm f}\end{pmatrix}$$

Hull contribution to added mass and inertia. Suppose we fix a body reference frame in the spheroid principal axes such that the x-axis is the hull's axis of rotational symmetry. Let a denote the semi-axis length of the x-axis and let b denote the semi-axis length of the body y- and z-axes. For a prolate spheroid, $a>b$. The mass of fluid displaced by the body is

$$\bar{m}=\frac{4}{3}\pi\rho ab^2.$$

Define the spheroid eccentricity

$$e=\sqrt{1-\left(\frac{b}{a}\right)^2}$$

and define constants

$$\begin{aligned}\tilde{a} &= \frac{2(1-e^2)}{e^3}\left(\frac{1}{2}\ln\frac{1+e}{1-e} - e\right)\\ \tilde{b} &= \frac{1}{e^2} - \frac{1-e^2}{2e^3}\ln\frac{1+e}{1-e}.\end{aligned}$$

The generalized added inertia matrix for the spheroidal hull is

$$\mathbb{M}_{\mathrm{f_h}} = \begin{pmatrix} \boldsymbol{M}_{\mathrm{f_h}} & \mathbf{0} \\ \mathbf{0} & \boldsymbol{I}_{\mathrm{f_h}} \end{pmatrix}$$

where

$$\boldsymbol{M}_{\mathrm{f_h}} = \mathrm{diag}\ (m_{\mathrm{h}_x}, m_{\mathrm{h}_z}, m_{\mathrm{h}_z}) \qquad \text{and} \qquad \boldsymbol{I}_{\mathrm{f_h}} = \mathrm{diag}\ (I_{\mathrm{h}_{xx}}, I_{\mathrm{h}_{zz}}, I_{\mathrm{h}_{zz}})$$

The nonzero components of the hull added mass matrix $\boldsymbol{M}_{\mathrm{f_h}}$ are

$$m_{\mathrm{h}_x} = \left(\frac{\tilde{\alpha}}{2-\tilde{\alpha}}\right)m \qquad \text{and} \qquad m_{\mathrm{h}_y} = m_{\mathrm{h}_z} = \left(\frac{\tilde{b}}{2-\tilde{b}}\right)m.$$

The components of the hull added inertia matrix $\boldsymbol{I}_{\mathrm{f_h}}$ are

$$I_{\mathrm{h}_{xx}} = 0 \qquad \text{and} \qquad I_{\mathrm{h}_{yy}} = I_{\mathrm{h}_{zz}} = \frac{m}{5}\frac{(b^2-a^2)^2(\tilde{a}-\tilde{b})}{2(b^2-a^2)-(b^2+a^2)(\tilde{a}-\tilde{b})}.$$

Control plane contributions to added mass and inertia. The four control planes are located at the stern of the vehicle in a cruciform configuration. We model each plane as an "all-moving surface" that provides attitude stability and control in forward motion. We label the fins as follows:

1. Dorsal control plane
2. Starboard control plane
3. Ventral control plane
4. Port control plane

Control plane deflections d_i ($i \in \{1,2,3,4\}$) are defined to be positive in the counterclockwise direction when viewed "end-on." Equivalently, the sign convention is defined by a right-hand rule about each control plane's pivot axis, pointing *outward* from the vehicle centerline.

Assuming that the control planes are located very near the tail of the vehicle, we may estimate the added mass of a given control plane as

$$m_{\mathrm{p}} = \frac{\rho\pi}{4AR_{\mathrm{p}}} b_{\mathrm{p}} S_{\mathrm{p}}$$

where b_{p} is the control plane semi-span, measured from the hull axis of symmetry to the tip of the plane, and S_{p} is the control plane area. The control plane's *aspect ratio* is

$$AR_{\mathrm{p}} = \frac{b_{\mathrm{p}}^2}{S_{\mathrm{p}}}$$

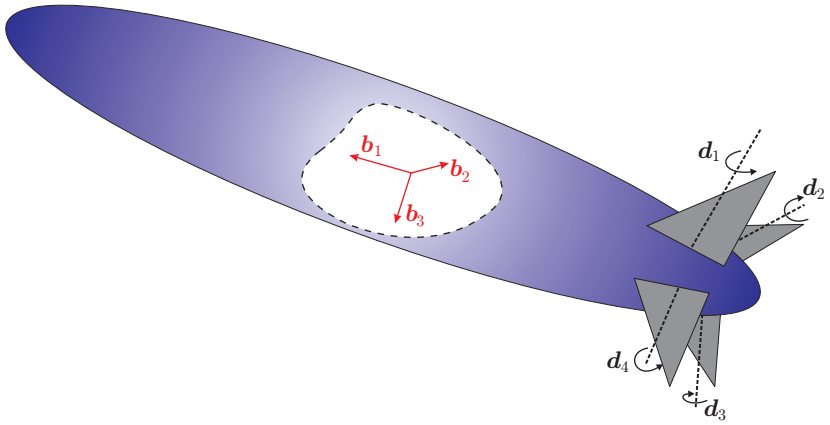

Figure 7: Naming and sign convention for control planes.

For a rectangular fin, the control plane chord is

$$c_{\mathrm{p}} = \frac{S_{\mathrm{p}}}{b_{\mathrm{p}}}$$

in which case the aspect ratio is simply the ratio of the semi-span to the chord

$$AR_{\mathrm{p}} = \frac{b_{\mathrm{p}}}{c_{\mathrm{p}}}$$

with large values corresponding to "long, narrow" control planes.

The matrix representing the added mass contributions from the control planes is

$$\boldsymbol{M}_{\mathrm{f_p}} = \mathrm{diag}\ \left(m_{\mathrm{p}_x}, m_{\mathrm{p}_y}, m_{\mathrm{p}_z}\right)$$

where

$$\begin{aligned}
m_{\mathrm{p}_x} &= m_{\mathrm{p}}\left(\sin d_1 + \sin d_2 + \sin d_3 + \sin d_4\right) && \approx m_{\mathrm{p}}\left(d_1 + d_2 + d_3 + d_4\right) \\
m_{\mathrm{p}_y} &= m_{\mathrm{p}}\left(\cos d_1 + \cos d_3\right) && \approx 2m_{\mathrm{p}} \\
m_{\mathrm{p}_z} &= m_{\mathrm{p}}\left(\cos d_2 + \cos d_4\right) && \approx 2m_{\mathrm{p}}
\end{aligned}$$

Here, we assume that the deflections are small and we ignore the coupling that arises due to control deflections. (If $d_1 = -d_3 > 0$ with $d_2 = d_4 = 0$, for example, there would be a small sway force due to surge acceleration and, likewise, a small surge force due to sway acceleration; we ignore such coupling effects.)

Assuming that the center of lift of each control plane is located a distance $x_{\mathrm{p}} > 0$ aft of the hull's geometric center and a distance $z_{\mathrm{p}} > 0$ off of the centerline, the matrix representing the added inertia contributions from the control planes is

$$\boldsymbol{I}_{\mathrm{f_p}} = \mathrm{diag}\ \left(I_{\mathrm{p}_{xx}}, I_{\mathrm{p}_{zz}}, I_{\mathrm{p}_{zz}}\right)$$

where

$$\begin{aligned}
I_{\mathrm{p}_{xx}} &= \left(m_{\mathrm{p}} z_{\mathrm{p}}^2\right)\left(\cos d_1 + \cos d_2 + \cos d_3 + \cos d_4\right) && \approx 4m_{\mathrm{p}} z_{\mathrm{p}}^2 \\
I_{\mathrm{p}_{yy}} &= \left(m_{\mathrm{p}} x_{\mathrm{p}}^2\right)\left(\cos d_2 + \cos d_4\right) && \approx 2m_{\mathrm{p}} x_{\mathrm{p}}^2 \\
I_{\mathrm{p}_{zz}} &= \left(m_{\mathrm{p}} x_{\mathrm{p}}^2\right)\left(\cos d_1 + \cos d_3\right) && \approx 2m_{\mathrm{p}} x_{\mathrm{p}}^2
\end{aligned}$$

Again, we ignore added inertia coupling that arises due to deflections.

The fact that the control planes are offset from the spheroidal hull's principal axes means, in addition to added mass and inertia, these surfaces contribute hydrodynamic coupling between translational and rotational motions. The effects are characterized by the coupling matrix

$$\boldsymbol{C}_{\mathrm{f_p}} = \begin{pmatrix} 0 & 0 & 0 \\ 0 & 0 & C_{\mathrm{p23}} \\ 0 & C_{\mathrm{p32}} & 0 \end{pmatrix}$$

where

$$\begin{aligned} C_{\mathrm{p23}} &= (m_{\mathrm{p}} x_{\mathrm{p}})\,(\cos d_1 + \cos d_3) && \approx 2 m_{\mathrm{p}} x_{\mathrm{p}} \\ C_{\mathrm{p32}} &= (m_{\mathrm{p}} x_{\mathrm{p}})\,(-\cos d_2 - \cos d_4) && \approx -2 m_{\mathrm{p}} x_{\mathrm{p}} \end{aligned}$$

The term C_{p23} determines the sway force due to yaw acceleration and the term C_{p32} represents the heave force due to pitch acceleration. Because the vertical control planes are located at the stern, a positive (nose right) yaw acceleration results in a positive sway force and a positive (nose up) pitch acceleration results in a negative heave force.

Complete added mass and inertia. Summing added mass contributions from the hull and appendages we have

$$\boldsymbol{M}_{\mathrm{f}} = \boldsymbol{M}_{\mathrm{f_h}} + \boldsymbol{M}_{\mathrm{f_p}} = \mathrm{diag}(m_x, m_y, m_z)$$

where

$$\begin{aligned} m_x &\approx m_{\mathrm{h}_x} && = \left(\frac{\tilde{a}}{2-\tilde{a}}\right) m \\ m_y &= m_{\mathrm{h}_y} + m_{\mathrm{p}_y} = \left(\frac{\tilde{b}}{2-\tilde{b}}\right) m + 2 m_{\mathrm{p}} \\ m_z &= m_{\mathrm{h}_z} + m_{\mathrm{p}_z} = \left(\frac{\tilde{b}}{2-\tilde{b}}\right) m + 2 m_{\mathrm{p}} \end{aligned}$$

Here, we have assumed that we may ignore the effect of small control plane deflections on the surge added mass: $m_{\mathrm{h}_x} \gg m_{\mathrm{p}_x}$.

The added inertia is

$$\boldsymbol{I}_{\mathrm{f}} = \boldsymbol{I}_{\mathrm{f_h}} + \boldsymbol{I}_{\mathrm{f_p}} = \mathrm{diag}(I_{xx}, I_{yy}, I_{zz})$$

where

$$\begin{aligned} I_{xx} &= I_{\mathrm{h}_{xx}} + I_{\mathrm{p}_{xx}} = 4 m_{\mathrm{p}} z_{\mathrm{p}}^2 \\ I_{yy} &= I_{\mathrm{h}_{yy}} + I_{\mathrm{p}_{yy}} = \frac{m}{5}\left(\frac{(b^2-a^2)^2(\tilde{a}-\tilde{b})}{2(b^2-a^2)-(b^2+a^2)(\tilde{a}-\tilde{b})}\right) + 2 m_{\mathrm{p}} x_{\mathrm{p}}^2 \\ I_{zz} &= I_{\mathrm{h}_{zz}} + I_{\mathrm{p}_{zz}} = \frac{m}{5}\left(\frac{(b^2-a^2)^2(\tilde{a}-\tilde{b})}{2(b^2-a^2)-(b^2+a^2)(\tilde{a}-\tilde{b})}\right) + 2 m_{\mathrm{p}} x_{\mathrm{p}}^2 \end{aligned}$$

The hydrodynamic coupling matrix is

$$\boldsymbol{C}_{\mathrm{f}} = \boldsymbol{C}_{\mathrm{f_p}} \approx \boldsymbol{C}_{\mathrm{f_p}} = \begin{pmatrix} 0 & 0 & 0 \\ 0 & 0 & 2 m_{\mathrm{p}} x_{\mathrm{p}} \\ 0 & -2 m_{\mathrm{p}} x_{\mathrm{p}} & 0 \end{pmatrix}$$

Gravity and buoyancy effects. Because the body is neutrally buoyant, there is no net gravitational force. However, there will be a moment due to gravity and buoyancy, in general. For the given choice of body reference frame,

$$\boldsymbol{m}_{\mathrm{g/b}} = \boldsymbol{r}_{\mathrm{cm}} \times mg\boldsymbol{R}^T\boldsymbol{i}_3$$

Given that the origin of the body frame is the center of buoyancy, we let $\boldsymbol{r}_{\mathrm{cm}} = [0, 0, \gamma]^T$ with $\gamma > 0$. In this case, gravity provides a stabilizing moment about the pitch and roll axes.

Viscous effects. The viscous force and moment are also given in terms of the contribution from the hull and the contributions from the control planes. These forces and moments depend on the hydrodynamic angles

$$\alpha = \arctan\left(\frac{u_{\mathrm{r}}}{w_{\mathrm{r}}}\right) \qquad \text{and} \qquad \beta = \arctan\left(\frac{v_{\mathrm{r}}}{\|\boldsymbol{v}_{\mathrm{r}}\|}\right)$$

These angles describe the orientation of the vehicle with respect to its flow-relative velocity vector vector. Accordingly, one may define a map from the so-called "current frame" (or "wind frame" in aircraft dynamics vocabulary) to the body-fixed reference frame:

$$\boldsymbol{R}_{\mathrm{BW}} = \exp\left(-\alpha\hat{\boldsymbol{e}}_2\right)\exp\left(\beta\hat{\boldsymbol{e}}_3\right)$$

where $\boldsymbol{e}_j$ is the j^{th} basis vector for $\mathbb{R}^n$.

Considering first the hull, we define S_{h} to be the frontal area and we define the dynamic pressure

$$P_{\mathrm{dyn}} = \frac{1}{2}\rho\|\boldsymbol{v}_{\mathrm{r}}\|^2$$

With these definitions, we have

$$\begin{aligned}
\boldsymbol{f}_{\mathrm{v_h}} &= -P_{\mathrm{dyn}}S_{\mathrm{h}}\boldsymbol{R}_{\mathrm{BW}}(\alpha,\beta)\begin{pmatrix} C_{D_{\mathrm{h}}}(\alpha,\beta) \\ C_{SF_{\mathrm{h}}}(\beta) \\ C_{L_{\mathrm{h}}}(\alpha) \end{pmatrix} \\
\boldsymbol{m}_{\mathrm{v_h}} &= -\boldsymbol{D}_{\omega}\boldsymbol{\omega}_r
\end{aligned}$$

where

$$\begin{pmatrix} C_{D_{\mathrm{h}}}(\alpha,\beta) \\ C_{SF_{\mathrm{h}}}(\beta) \\ C_{L_{\mathrm{h}}}(\alpha) \end{pmatrix} = \begin{pmatrix} C_{D_{0_{\mathrm{h}}}} + C_{D_{1_{\mathrm{h}}}}\left(1 - \cos\left(2\sqrt{\alpha^2+\beta^2}\right)\right) \\ C_{L_{\alpha_{\mathrm{h}}}}\beta \\ C_{L_{\alpha_{\mathrm{h}}}}\alpha \end{pmatrix}$$

and where

$$\boldsymbol{D}_{\omega_{\mathrm{h}}} = \mathrm{diag}\ \left(0, d_{\omega_{\mathrm{h}}}, d_{\omega_{\mathrm{h}}}\right)$$

The constants appearing in these expressions ($C_{D_{0_{\mathrm{h}}}}$, $C_{D_{1_{\mathrm{h}}}}$, $C_{L_{\alpha_{\mathrm{h}}}}$, and $d_{\omega_{\mathrm{h}}}$) may be obtained experimentally.

Next, we consider the effect of the control planes. Like the hull, the control planes exert forces that are functions of the vehicle angle of attack α and sideslip angle β as well as the control plane deflections d_i. The hydrodynamic angle that the control planes experience is also a function of the vehicle's angular rate, as the body's rotation causes an effective change in the flow angles at the tail. Accordingly, we define the angles

$$\begin{aligned}
\alpha_q &= \frac{q_{\mathrm{r}}x_{\mathrm{p}}}{u_{\mathrm{r}}} & \beta_r &= -\frac{r_{\mathrm{r}}x_{\mathrm{p}}}{u_{\mathrm{r}}} \\
\alpha_p &= \frac{p_{\mathrm{r}}z_{\mathrm{p}}}{u_{\mathrm{r}}} & \beta_p &= \frac{p_{\mathrm{r}}z_{\mathrm{p}}}{u_{\mathrm{r}}}
\end{aligned}$$

With these definitions, we write

$$\begin{aligned}
\boldsymbol{f}_{\mathrm{v_p}} &= P_{\mathrm{dyn}} S_{\mathrm{p}} \boldsymbol{R}_{\mathrm{BW}}(\alpha,\beta) \begin{pmatrix} -C_{D_{\mathrm{p}}} \\ C_{L_{\mathrm{p_1}}} + C_{L_{\mathrm{p_3}}} \\ C_{L_{\mathrm{p_2}}} + C_{L_{\mathrm{p_4}}} \end{pmatrix} \\
\boldsymbol{m}_{\mathrm{v_p}} &= P_{\mathrm{dyn}} S_{\mathrm{p}} \begin{pmatrix} z_{\mathrm{p}} \left(C_{L_{\mathrm{p_1}}} + C_{L_{\mathrm{p_2}}} - C_{L_{\mathrm{p_3}}} - C_{L_{\mathrm{p_4}}} \right) \\ x_{\mathrm{p}} \left(C_{L_{\mathrm{p_2}}} + C_{L_{\mathrm{p_4}}} \right) \\ -x_{\mathrm{p}} \left(C_{L_{\mathrm{p_1}}} + C_{L_{\mathrm{p_3}}} \right) \end{pmatrix}
\end{aligned}$$

where

$$C_{D_{\mathrm{p}}} = \frac{1}{\pi \mathcal{AR}_{\mathrm{p}}} \left(C_{L_{\mathrm{p_1}}}^2 + C_{L_{\mathrm{p_2}}}^2 + C_{L_{\mathrm{p_3}}}^2 + C_{L_{\mathrm{p_4}}}^2 \right)$$

and

$$\begin{aligned}
C_{L_{\mathrm{p_1}}} &= -C_{L_{\alpha_{\mathrm{p}}}} \left(d_1 + (\beta + \beta_r + \beta_p) \right) \\
C_{L_{\mathrm{p_2}}} &= -C_{L_{\alpha_{\mathrm{p}}}} \left(d_2 + (\alpha + \alpha_q + \alpha_p) \right) \\
C_{L_{\mathrm{p_3}}} &= -C_{L_{\alpha_{\mathrm{p}}}} \left(-d_3 + (\beta + \beta_r - \beta_p) \right) \\
C_{L_{\mathrm{p_4}}} &= -C_{L_{\alpha_{\mathrm{p}}}} \left(-d_4 + (\alpha + \alpha_q - \alpha_p) \right)
\end{aligned}$$

Note that the control planes are an essential contributor to the vehicle's angular rate damping, due to the angle of attack corrections α_q and α_p and the sideslip corrections β_r and β_p.

Summing the contributions from the hull and the fins, we have

$$\begin{aligned}
\boldsymbol{f}_{\mathrm{v}} &= \boldsymbol{f}_{\mathrm{v_h}} + \boldsymbol{f}_{\mathrm{v_f}} \\
\boldsymbol{m}_{\mathrm{v}} &= \boldsymbol{m}_{\mathrm{v_h}} + \boldsymbol{m}_{\mathrm{v_f}}
\end{aligned}$$

Propulsion and control effects. We account for propulsion and control effects separately, through the control force $\boldsymbol{f}_{\mathrm{ctrl}}$ and the control moment $\boldsymbol{m}_{\mathrm{ctrl}}$. The control forces and moments are typically generated using external effectors (e.g., propulsors and control planes) which alter the viscous force and moment, however these effects can be separated from the remaining viscous effects $\boldsymbol{f}_{\mathrm{v}}$ and $\boldsymbol{m}_{\mathrm{v}}$ to illuminate the role of actuation and to simplify the control design process.

Control plane deflections are more easily interpreted using standard notation from aircraft dynamics. We define the terms δa, δe, and δr to denote *effective aileron, elevator and rudder* deflections, respectively. The deflections are defined such that a positive value yields a positive moment about the corresponding axis. That is, $\delta a > 0$ yields a positive roll moment, $\delta e > 0$ yields a positive pitch moment, and $\delta r > 0$ yields a positive roll moment. Given the existing sign convention for control plane deflections d_i, we have

$$\begin{pmatrix} \delta a \\ \delta e \\ \delta r \end{pmatrix} = \begin{pmatrix} 0 & -1 & 0 & -1 \\ 0 & -1 & 0 & 1 \\ 1 & 0 & -1 & 0 \end{pmatrix} \begin{pmatrix} d_1 \\ d_2 \\ d_3 \\ d_4 \end{pmatrix}$$

In practice, a given feedback control structure would generate desired values for the aileron, elevator, and rudder angles. These can be converted to control plane deflections using the pseudoinverse:

$$\begin{pmatrix} d_1 \\ d_2 \\ d_3 \\ d_4 \end{pmatrix} = \frac{1}{2} \begin{pmatrix} 0 & 0 & 1 \\ -1 & -1 & 0 \\ 0 & 0 & -1 \\ -1 & 1 & 0 \end{pmatrix} \begin{pmatrix} \delta a \\ \delta e \\ \delta r \end{pmatrix}$$

Complete force and moment model. Summing the force and moment contributions for a neutrally buoyant vehicle, we have

$$\begin{aligned} \boldsymbol{f} &= \boldsymbol{f}_{\mathrm{v}} + \boldsymbol{f}_{\mathrm{ctrl}} \\ \boldsymbol{m} &= \boldsymbol{m}_{\mathrm{g/b}} + \boldsymbol{m}_{\mathrm{v}} + \boldsymbol{m}_{\mathrm{ctrl}} \end{aligned}$$

Linearized Dynamics. With conventional assumptions concerning symmetry of the vehicle, a constant propulsive force acting along the surge axis results in a steady motion of the form

$$\tilde{\boldsymbol{\nu}}_{\mathrm{r}} = \begin{pmatrix} \tilde{u}_{\mathrm{r}} \\ 0 \\ 0 \end{pmatrix} \qquad \text{and} \qquad \tilde{\boldsymbol{\omega}} = \boldsymbol{0}$$

In this condition, thrust is balanced drag ($\boldsymbol{f}_{\mathrm{v}} + \boldsymbol{f}_{\mathrm{ctrl}} = \boldsymbol{0}$) and no control moment is required ($\boldsymbol{m}_{\mathrm{ctrl}} = \boldsymbol{0}$) to maintain the steady motion. Determining the *stability* of the steady motion requires analyzing the vehicle's response to small perturbations. Linearizing about the steady motion above yields the small perturbation equations

$$\begin{pmatrix} \boldsymbol{M} & \boldsymbol{C} \\ \boldsymbol{C}^T & \boldsymbol{I} \end{pmatrix} \begin{pmatrix} \Delta\dot{\boldsymbol{\nu}}_{\mathrm{r}} \\ \Delta\dot{\boldsymbol{\omega}} \end{pmatrix} = \begin{pmatrix} \boldsymbol{0} & -\widehat{\tilde{\boldsymbol{\nu}}}_{\mathrm{r}}\boldsymbol{C} + \widehat{\boldsymbol{M}\tilde{\boldsymbol{\nu}}}_{\mathrm{r}} \\ \left(\widehat{\boldsymbol{M}\tilde{\boldsymbol{\nu}}}_{\mathrm{r}} - \hat{\tilde{\boldsymbol{\nu}}}_{\mathrm{r}}\boldsymbol{M}\right) & \widehat{\boldsymbol{C}^T\tilde{\boldsymbol{\nu}}}_{\mathrm{r}} \end{pmatrix} \begin{pmatrix} \Delta\boldsymbol{\nu}_{\mathrm{r}} \\ \Delta\boldsymbol{\omega} \end{pmatrix} + \begin{pmatrix} \Delta\boldsymbol{f} \\ \Delta\boldsymbol{m} \end{pmatrix} \tag{25}$$

where $\Delta\boldsymbol{\nu}_{\mathrm{r}} = \boldsymbol{\nu}_{\mathrm{r}} - \tilde{\boldsymbol{\nu}}_{\mathrm{r}}$ and $\Delta\boldsymbol{\omega} = \boldsymbol{\omega} - \tilde{\boldsymbol{\omega}}$.

Given that the origin of the body frame is the center of buoyancy, if we let $\boldsymbol{r}_{\mathrm{cm}} = [0, 0, \gamma]^T$ with $\gamma > 0$, then gravity will provide a stabilizing moment about the pitch and roll axes.

For illustrative purposes, we focus on the dynamics of an underwater vehicle moving in the horizontal plane. In this case, with conventional assumptions concerning vehicle symmetry, the six degree of freedom motion decouples into two independent subsystems: diving and steering.

Incorporating the pitch kinematics, the linearized diving dynamics are described by the following system of equations

$$\begin{aligned} &\begin{pmatrix} 1 & 0 & 0 & 0 \\ 0 & m_x & 0 & m\gamma \\ 0 & 0 & m_z & -2m_{\mathrm{p}}x_{\mathrm{p}} \\ 0 & m\gamma & -2m_{\mathrm{p}}x_{\mathrm{p}} & I_{yy} \end{pmatrix} \begin{pmatrix} \Delta\dot{\theta} \\ \Delta\dot{u}_{\mathrm{r}} \\ \Delta\dot{w}_{\mathrm{r}} \\ \Delta\dot{q} \end{pmatrix} \\ &= \begin{pmatrix} 0 & 0 & 0 & 1 \\ 0 & \tilde{X}_u & 0 & 0 \\ 0 & 0 & Z_w & Z_q + m_x\tilde{u}_{\mathrm{r}} \\ -mg\gamma & 0 & M_w + (m_z - m_x)\tilde{u}_{\mathrm{r}} & M_q - 2m_{\mathrm{p}}x_{\mathrm{p}}\tilde{u}_{\mathrm{r}} \end{pmatrix} \begin{pmatrix} \Delta\theta \\ \Delta u_{\mathrm{r}} \\ \Delta w_{\mathrm{r}} \\ \Delta q \end{pmatrix} + \begin{pmatrix} 0 & 0 \\ X_{\delta T} & 0 \\ 0 & Z_{\delta e} \\ 0 & M_{\delta e} \end{pmatrix} \begin{pmatrix} \delta T \\ \delta e \end{pmatrix} \end{aligned} \tag{26}$$

where δT and δe are the deviations of the throttle and elevator inputs from their nominal values, respectively. The overtilde on the term $\tilde{X}_u$ is intended to distinguish it from the zero-speed linear surge damping coefficient, which is conventionally denoted X_u. For our system, we have

$$\tilde{X}_u \approx \rho\tilde{u}_{\mathrm{r}}S_{\mathrm{h}}C_{D_{0_{\mathrm{h}}}}$$

Approximations for other stability derivatives, in terms of previous definitions, are given below:

$$
\begin{aligned}
Z_w &\approx -\frac{1}{2}\rho\tilde{u}_{\mathrm{r}}\left(S_{\mathrm{h}}\left(C_{L_{\alpha_{\mathrm{h}}}}+C_{D_{0_{\mathrm{h}}}}\right)+S_{\mathrm{p}}\left(2C_{L_{\alpha_{\mathrm{p}}}}\right)\right) & M_w &\approx -\rho\tilde{u}_{\mathrm{r}}S_{\mathrm{p}}C_{L_{\alpha_{\mathrm{p}}}}x_{\mathrm{p}}\\
Z_q &\approx -\rho\tilde{u}_{\mathrm{r}}S_{\mathrm{p}}C_{L_{\alpha_{\mathrm{p}}}}x_{\mathrm{p}} & M_q &\approx -\rho\tilde{u}_{\mathrm{r}}S_{\mathrm{p}}C_{L_{\alpha_{\mathrm{p}}}}x_{\mathrm{p}}^2\\
Z_{\delta e} &\approx \rho\tilde{u}_{\mathrm{r}}^2S_{\mathrm{p}}C_{L_{\alpha_{\mathrm{p}}}} & M_{\delta e} &\approx \rho\tilde{u}_{\mathrm{r}}^2S_{\mathrm{p}}\left(C_{L_{\alpha_{\mathrm{p}}}}x_{\mathrm{p}}\right)
\end{aligned}
$$

Incorporating the roll kinematics, the linearized steering dynamics are described by the following system of equations

$$
\begin{aligned}
&\begin{pmatrix} 1 & 0 & 0 & 0\\ 0 & m_y & -m\gamma & 2m_{\mathrm{p}}x_{\mathrm{p}}\\ 0 & -m\gamma & I_{xx} & 0\\ 0 & 2m_{\mathrm{p}}x_{\mathrm{p}} & 0 & I_{zz}\end{pmatrix}\begin{pmatrix}\Delta\dot{\phi}\\ \Delta\dot{v}_{\mathrm{r}}\\ \Delta\dot{p}\\ \Delta\dot{r}\end{pmatrix}\\
&=\begin{pmatrix} 0 & 0 & 1 & 0\\ 0 & Y_v & 0 & Y_r-m_x\tilde{u}_{\mathrm{r}}\\ -mg\gamma & 0 & K_p & m\gamma\tilde{u}_{\mathrm{r}}\\ 0 & N_v+(m_x-m_y)\tilde{u}_{\mathrm{r}} & 0 & N_r-2m_{\mathrm{p}}x_{\mathrm{p}}\end{pmatrix}\begin{pmatrix}\Delta\phi\\ \Delta v_{\mathrm{r}}\\ \Delta p\\ \Delta r\end{pmatrix}+\begin{pmatrix} 0 & 0\\ 0 & Y_{\delta r}\\ K_{\delta a} & 0\\ 0 & N_{\delta r}\end{pmatrix}\begin{pmatrix}\delta a\\ \delta r\end{pmatrix}
\end{aligned}
\tag{27}
$$

The stability derivatives are:

$$
\begin{aligned}
K_p &\approx -2\rho\tilde{u}_{\mathrm{r}}S_{\mathrm{p}}C_{L_{\alpha_{\mathrm{p}}}}z_{\mathrm{p}} & K_{\delta a} &\approx 2\rho\tilde{u}_{\mathrm{r}}^2S_{\mathrm{p}}C_{L_{\alpha_{\mathrm{p}}}}z_{\mathrm{p}}\\
Y_v &= Z_w & N_v &= -M_w\\
Y_r &= -Z_q & N_r &= M_q\\
Y_{\delta r} &= -Z_{\delta e} & N_{\delta r} &= M_{\delta e}
\end{aligned}
\tag{28}
$$

Feedback control. A simple and effective approach to feedback control of a slender AUV is proportional-derivative (PD) control of the vehicle angles

$$
\begin{aligned}
\delta a &= -k_{p_\phi}\phi-k_{d_\phi}p\\
\delta e &= -k_{p_\theta}(\theta-\theta_{\mathrm{d}})-k_{d_\theta}q\\
\delta r &= -k_{p_\psi}(\psi-\psi_{\mathrm{d}})-k_{d_\psi}r
\end{aligned}
$$

The state variables used in the feedback structure defined above can be readily measured using standard sensors. Control system performance can be easily tuned for operation near a given nominal speed.